

 Open access • Posted Content • DOI:10.20944/PREPRINTS202010.0098.V1

In Silico Analysis of Some Phytochemicals as Potent Anti-tubercular Agents Targeting Mycobacterium tuberculosis RNA Polymerase and InhA Protein — Source link





Emran, Md. Mofijur Rahman, Afroza Khanam Anika, Sultana Hossain Nasrin ...+1 more authors

Published on: 05 Oct 2020

Topics: INH A, Mycobacterium tuberculosis and In silico

Related papers:

- [IN SILICO STUDY FOR IDENTIFICATION OF DRUG LIKE INHIBITOR FROM NATURAL COMPOUNDS AGAINST INHA REDUCTASE OF MYCOBACTERIUM TUBERCULOSIS](#) Original Article
- [Discovery of natural inhibitors targeting 2 - trans enoyl acyl carrier protein reductase in Mycobacterium tuberculosis by structure based drug designing](#)
- [Insights into comparative molecular docking study of selected novel thiophene derivative vs standard anti-tubercular drugs against Mycobacterium tuberculosis target enzymes](#)
- [Direct inhibitors of InhA are active against Mycobacterium tuberculosis](#)
- [Structure-based design of a novel class of potent inhibitors of InhA, the enoyl acyl carrier protein reductase from Mycobacterium tuberculosis: a computer modelling approach.](#)

Share this paper:    

View more about this paper here: <https://typeset.io/papers/in-silico-analysis-of-some-phytochemicals-as-potent-anti-18tqpp5l2i>

In Silico Analysis of Some Phytochemicals as Potent Anti-tubercular Agents Targeting *Mycobacterium tuberculosis* RNA Polymerase and InhA Protein

Md Emran¹ , Md. Mofijur Rahman¹ , Afroza Khanam Anika¹ , Sultana Hossain Nasrin¹ , Abu Tayab Moin^{2*}

¹Department of Biochemistry and Biotechnology, Faculty of Basic Medical and pharmaceutical Sciences, University of Science and Technology Chittagong, Chattogram, Bangladesh

²Department of Genetic Engineering and Biotechnology, Faculty of Biological Sciences University of Chittagong, Chattogram, Bangladesh

For Correspondence:

Abu Tayab Moin

Email: tayabmoin786@gmail.com

Abstract

Tuberculosis (TB) is a contagious disease, caused by *Mycobacterium tuberculosis* (MTB) that has infected and killed a lot of people in the past. At present treatments against TB are available at a very low cost. Since these chemical drugs have many adverse effects on health, more attention is now given on the plant-derived phytochemicals as potential agents to fight against TB. In this study, 5 phytochemicals, 4-hydroxybenzaldehyde, benzoic acid, bergapten, psoralen, and p-hydroxybenzoic acid, are selected to test their potentiality, safety, and efficacy against two

potential targets, the MTB RNA polymerase and enoyl-acyl carrier protein (ACP) reductase, the InhA protein, using various tools of in silico biology. The molecular docking experiment, drug-likeness property test, ADME/T-test, P450 SOM prediction, pharmacophore mapping, and modeling, solubility testing, DFT calculations, and PASS prediction study had confirmed that all the molecules had the good potentiality to inhibit the two targets. However, two agents, 4-hydroxybenzaldehyde and bergapten were considered as the best agents among the five selected agents and they also showed far better results than the two currently used drugs, that function in these pathways, rifampicin (MTB RNA polymerase) and isoniazid (InhA protein). These two agents can be used effectively to treat tuberculosis.

Keywords: Tuberculosis, 4-hydroxybenzaldehyde, bergapten, molecular docking.

1. Introduction

Tuberculosis (TB) is an ancient disease that plagued mankind many times in the past. It was responsible for many great epidemics. *Mycobacterium tuberculosis* (MTB) is the bacteria that is responsible for tuberculosis disease. This bacteria may have killed more people than any other microbial pathogens (Daniel, 2006). However, at present, tuberculosis is a preventable as well as a curable disease, which is possible at a very low cost. Tuberculosis is a highly contagious disease that can transmit via cough, spit, and sneezes of the infected person. MTB primarily infects the

lungs (. Grange and Zumla, 2002; Sepkowitz, 1996, Shah et al., 2015). If the disease is found in the lungs, then it is called pulmonary TB. However, TB can be found at other locations of the body. Such TB is called extra-pulmonary TB. Several antibiotics are used to fight against MTB. However, a new TB has emerged in recent years, which is resistant to multiple drugs that are commonly used in TB treatment. This new TB is called multidrug-resistant tuberculosis (MDR-TB). At present, rifampicin, isoniazid, pyrazinamide, and ethambutol are used all together to treat tuberculosis. However, as the MDR-TB is found to be resistant to multiple drugs that are used in the treatment of normal TB, other sets of drugs are used to treat the MDR-TB (Sreeramareddy et al., 2008; McIlleron et al., 2006; Ettehad et al., 2012). Rifampicin inhibits bacterial growth by inhibiting the RNA polymerase enzyme. RNA polymerase enzyme is responsible for synthesizing an RNA strand from a DNA strand by the process known as transcription (**Figure 01**). Ethambutol exerts its effects by inhibiting the transfer of mycolic acids into the cell wall of MTB as well as by changing the lipid metabolism of the bacteria. Pyrazinamide disrupts the membrane energetics and membrane transport. Thus, pyrazinamide shortens TB therapy (Rastogi and David, 1993; Zhang et al., 2003). Isoniazid, a drug used for treating TB, inhibits bacterial growth by inhibiting InhA protein, an enoyl-acyl carrier protein (ACP) reductase. The InhA protein is involved in the type II fatty acid biosynthesis pathway as well as mycolic acid synthesis which is an essential component of the bacterial cell membrane (Ducasse-Cabanot et al., 2004; He et al., 2007). In the mycolic acid synthesis pathway, two types of fatty acid synthase (FAS) enzymes are involved: FAS I and FAS II. The FAS I enzyme generates the starting material of the mycolic acid synthesis, acetyl-CoA. The acyl-CoA is converted to 3-ketoacyl-ACP by Kas III enzyme (beta-ketoacyl-ACP synthase III). The 3-ketoacyl-ACP then enters into a cyclic reaction catalyzed by the FAS II enzyme. 3-ketoacyl-ACP is converted into 3R-hydroxyacyl-ACP by beta-ketoacyl-

ACP reductase enzyme, MabA. The 3R-hydroxyacyl-ACP is later converted to trans-2-enol-ACP by beta-hydroxyacyl-ACP dehydratases, HadAB and HadBC. Next, the trans-2-enol-ACP is converted to acetyl-ACP by the InhA protein. The acyl-ACP can be converted to either 3-ketoacyl-ACP to start the cycle again (catalyzed by beta-keto-acyl-ACP synthetases, KasA and KasB proteins), or it can be converted to higher chained ACP like C18-ACP and later the C18-ACP forms ever higher chained ACP like C48-ACP to C62-ACP. Moreover, FAS I also generates carboxylated C26-CoA, which together with C48-C62-ACP, undergoes condensation/reduction reaction and forms mycolic acid (**Figure 02**). The inhibitors of InhA enzyme acts by inhibiting InhA and thus prevents the mycolic acid synthesis (Dong et al., 2015; Molle et al., 2010; Carel et al., 2014).

Computational methods are now extensively used in drug R&D processes. Such virtual screening methods reduce both time and cost of the drug discovery and development processes. Computational simulation tools are used in designing more than 50 drugs to this date and many of them have received FDA approval. Molecular docking predicts the interaction, pose, and conformation of a ligand within the binding site of a target molecule. After estimating the interactions, the software assigns scores to each of the bound ligands with a specified algorithm which reflects the binding affinity. Lowest score of binding (lowest docking score) represents the most appreciable interaction between the ligand and receptor (Zoete et al., 2009; Schneidman-Duhovny et al., 2004).

Natural agents from plants like 4-hydroxybenzaldehyde, benzoic acid, bergapten, Psoralen, p-hydroxybenzoic acid and many other compounds are proved to exhibit anti-tuberculosis properties in various studies (Chen et al., 2005; Lim, 2014; Dokorou et al., 2004; Chiang et al., 2010; Chen, 2007). The agents can be extracted from a variety of plant sources (**Table 01**). In this experiment,

the two commercially available and mostly used drugs, rifampicin against MTB RNA polymerase and isoniazid against the InhA protein, were used as controls. The mentioned five ligands: 4-hydroxybenzaldehyde, benzoic acid, bergapten, psoralen and p-hydroxybenzoic acid, are used to dock against the MTB RNA polymerase and the InhA protein to test their efficacy and potentiality against the enzymes. Later, the two best ligands, each against one enzyme, were determined by analyzing the various tests that are conducted in the experiment and the two ligands were compared with the control to test their efficiency to inhibit TB.

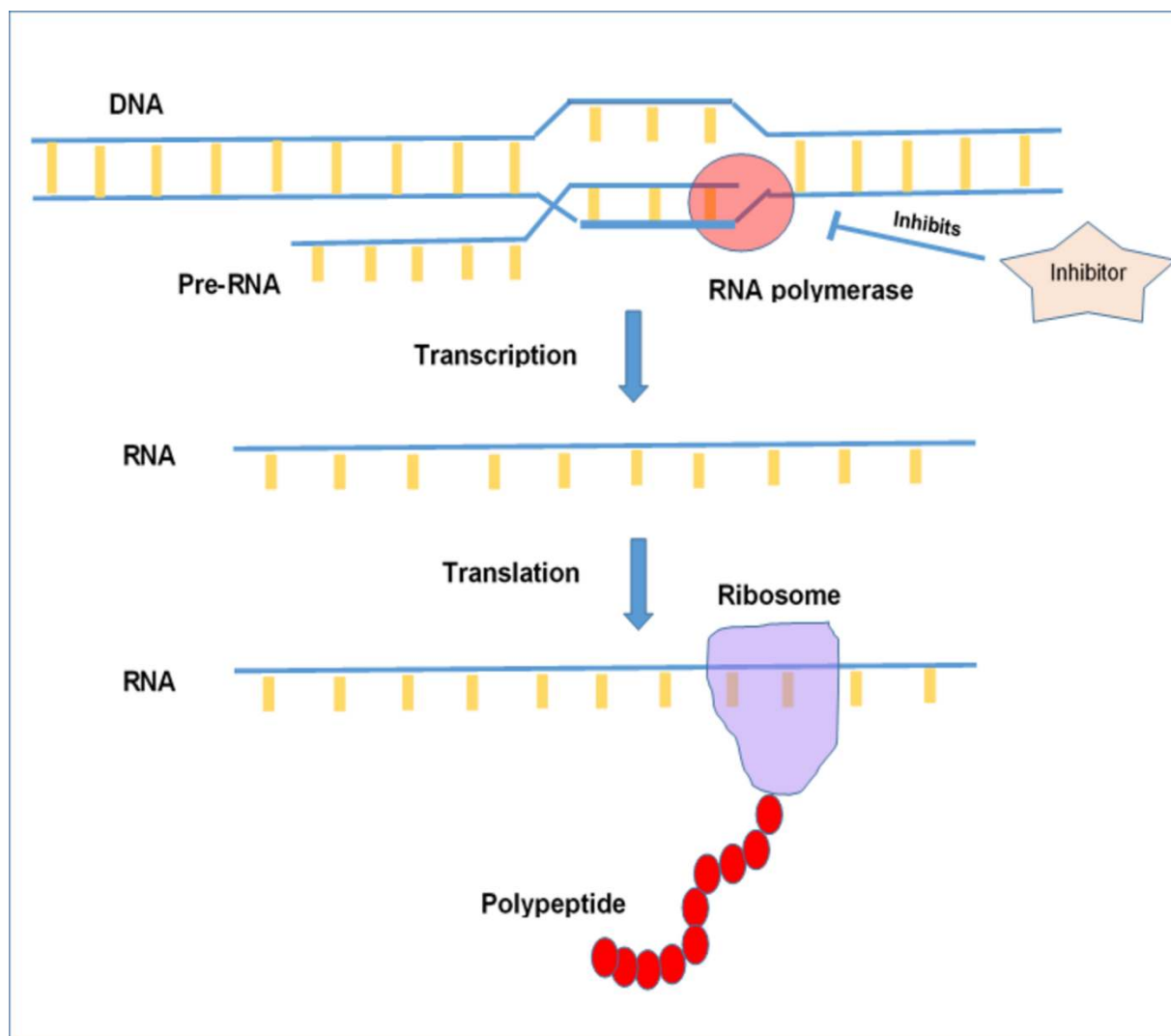


Figure 01. RNA polymerase is the enzyme that is responsible for the transcription of DNA to mRNA. Inhibiting RNA polymerase would result in disruption of transcription, which can be lethal to the cell and the organism.

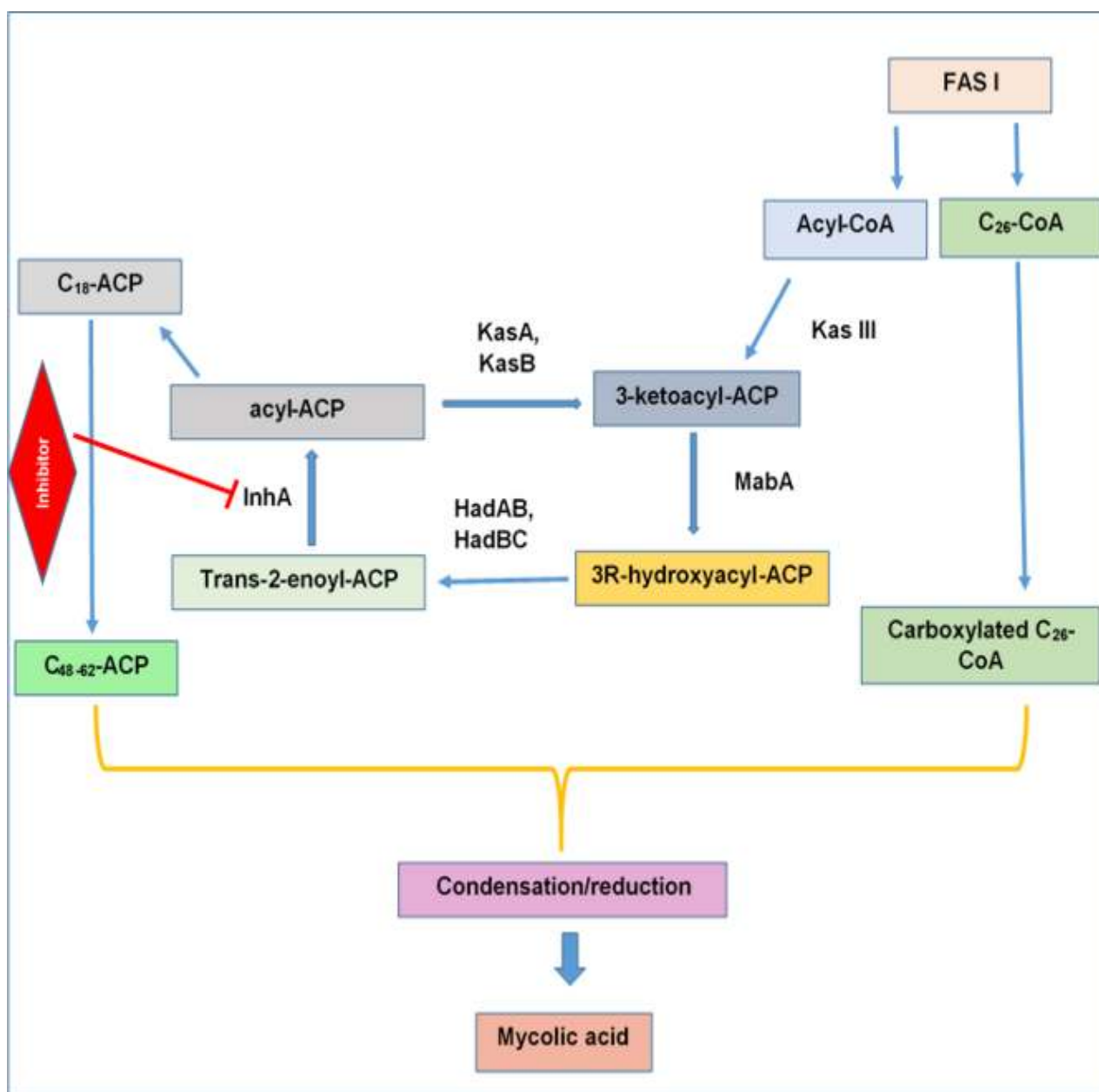


Figure 02. The involvement of InhA protein in the mycolic acid synthesis pathway. Here, FAS I and FAS II are fatty acid synthase I and II, respectively, MabA is a beta-ketoacyl-acyl carrier protein (ACP) reductase, HadAB and HadBC are beta-ketoacyl-ACP dehydratases, Kas A, Kas B and Kas III are beta-keto-acyl-ACP synthetases. Inhibitors of InhA protein can interfere with the formation of mycolic acid, which is an important component of MTB, thus inhibiting the MTB growth.

Table 01. Table showing anti-tuberculosis agents with their respective plant sources.

No	Name of the anti-tuberculosis agent	Plant source
01	4-hydroxybenzaldehyde	<i>Cinnamomum kotoense</i>
02	Benzoic acid	<i>Hibiscus taiwanensis</i>
03	Bergapten	<i>Fatoua pilosa</i>
04	Psoralen	<i>Fatoua pilosa</i>
05	p-hydroxybenzoic acid	<i>Microtropis fokienensis</i>

2. Materials and Methods

Ligand preparation, Grid generation and Glide docking, 2D representations of the best pose interactions between the ligands and their respective receptors were obtained using Maestro-Schrödinger Suite 2018-4 and the 3D representations of the best pose interactions between the ligands and their respective receptors were visualized using Discovery Studio Visualizer (Schrödinger Release 2015-1, 2015; Visualizer, 2017). The 2D structures of ligands were downloaded from PubChem in SDF format (www.pubchem.ncbi.nlm.nih.gov) and the two receptors were downloaded from protein data bank (www.rcsb.org).

2.1. Protein Preparation

Three-dimensional structure of MTB RNA polymerase (PDB ID: 6M7J) and InhA protein (PDB ID: 2NSD) were downloaded in PDB format from protein data bank (www.rcsb.org). The proteins were then prepared and refined using the Protein Preparation Wizard in Maestro Schrödinger Suite 2018-4 (Sastry et al., 2013). Bond orders were assigned and hydrogens were added to heavy atoms. Selenomethionines were converted to methionines as well as all the waters were deleted. Finally, the structure was optimized and then minimized using force field OPLS_2005.

2.2. Ligand Preparation and Receptor Grid Generation

The 2D conformations of 4-hydroxybenzaldehyde (PubChem CID: 126), Benzoic acid (PubChem CID: 243), Bergapten (PubChem CID: 2355), Psoralen (PubChem CID: 6199) and p-hydroxybenzoic acid (PubChem CID: 135) were downloaded (sequentially) from PubChem (www.pubchem.ncbi.nlm.nih.gov). The 3D conformers of the ligands were visualized by the Galaxy 3D Structure Generator v2018.01-beta tool of online server Molinspiration chemoinformatics (<https://www.molinspiration.com/>). These structures were then prepared using the LigPrep function of Maestro Schrödinger Suite 2018-4 (LigPrep, Schrödinger, 2014).

Grid usually confines the active site to shortened specific areas of the receptor protein for the ligand to dock specifically. In Glide, a grid was generated using default Van der Waals radius scaling factor 1.0 and charge cutoff 0.25 which was then subjected to the OPLS_2005 force field. A cubic box was generated around the active site (reference ligand active site). Then the grid box volume was adjusted to 15×15×15 for the docking test.

2.3. Glide Standard Precision (SP) Ligand Docking and MM-GBSA Prediction

SP adaptable glide docking was carried out using Glide in Maestro Schrödinger Suite 2018-4. The Van der Waals radius scaling factor and charge cutoff was set to 0.80 and 0.15 respectively for all

the ligand molecules. The ligand with the lowest glide docking score was considered as the best ligand. The 2D and 3D pose interactions between the ligands and receptor were visualized by Maestro Schrödinger Suite 2018-4 and the interaction of the ligand molecule with various types of amino acids as well as their bonds was analyzed by Discovery Studio Visualizer. The molecular mechanics- generalized born and surface area (MM-GBSA) tool was used to determine the ΔG_{Bind} scores. The MM-GBSA study was carried out using Maestro-Schrödinger Suite 2018-4.

2.4. Ligand Based Drug Likeness Property and ADME/Toxicity Prediction

The molecular structures of every ligand were analyzed using the SWISSADME server (<http://www.swissadme.ch/>) to confirm whether they obey Lipinski's rule of five or not, along with some other properties. Various physicochemical properties of ligand molecules were calculated using OSIRIS Property Explorer (<https://www.organic-chemistry.org/prog/peo/>). The drug-likeness properties of the selected ligand molecules were analyzed using the SWISSADME server (<http://www.swissadme.ch/>) as well as the OSIRIS Property Explorer (<https://www.organic-chemistry.org/prog/peo/>) (Organic Chemistry Portal. <https://www.organic-chemistry.org/prog/peo/>. 10/10/2019. Accessed: 09 August, 2019).

The ADME/T for each of the ligand molecules was carried out using online based servers, admetSAR (<http://lmmd.ecust.edu.cn/admetsar2/>) and ADMETlab (<http://admet.scbdd.com/>) to predict their various pharmacokinetic and pharmacodynamic properties. Both admetSAR and ADMETlab servers are comprehensive tools to determine the absorption, distribution, metabolism, excretion and toxicity of various chemical compounds (Cheng et al., 2014; Dong et al., 2018).

2.5. P450 Site of Metabolism (SOM) Prediction

The P450 Site of Metabolism (SOM) of the selected ligand molecules was determined by an online tool, RS-WebPredictor 1.0 (<http://reccr.chem.rpi.edu/Software/RS-WebPredictor/>) (Zaretzki et al.,

2012). The potential sites of metabolism on the selected ligands were determined for nine isoforms of the CYP 450 enzyme family: CYPs 1A2, 2A6, 2B6, 2C19, 2C8, 2C9, 2D6, 2E1 and 3A4.

2.6. Pharmacophore Modelling

The pharmacophore modelling of the 5 ligands was carried out using the Phase pharmacophore perception engine of Maestro-Schrödinger Suite 2018-4. The pharmacophore modelling was done manually. To carry out the process, the radii sizes were kept as the van der Waals radii of receptor atoms, the radii scaling factor was kept at 0.50, receptor atoms whose surfaces are within 2.00 Å of the ligand surface were ignored and the volume shell thickness was limited to 5.00 Å. The 2D and 3D pharmacophore modelling were carried out for all the ligand molecules.

2.7. Solubility Prediction

The solubility testing of the five ligands was performed using the QikProp wizard of Maestro-Schrödinger Suite 2018-4. In solubility prediction, the solubility of the selected ligands were determined in various interfaces like hexadecane/gas interface, octanol/gas interface, octanol/water interface etc.

2.8. DFT Calculation

Minimized ligand structures obtained from LigPrep were used for DFT calculation using the Jaguar panel of Maestro Schrödinger Suite v11.4 using Becke's three-parameter exchange potential and Lee-Yang-Parr correlation functional (B3LYP) theory with 6-31G* basis set (Lee et al., 1988; Becke, 1988). Quantum chemical properties such as surface properties (MO, density, potential) and Multipole moments were calculated along with HOMO (Highest Occupied Molecular Orbital) and LUMO (Lowest Unoccupied Molecular Orbital) energy. Then the global frontier orbital was analyzed and the hardness (η) and softness (S) of selected molecules were

calculated using the following equation as per Parr and Pearson interpretation and Koopmans theorem (Pearson, 1986; Parr et al., 1989).

$$\eta = (\text{HOMO} - \text{LUMO})/2,$$

$$S = 1/\eta$$

2.09. PASS (Prediction of Activity Spectra for Substances) Prediction Study

The PASS (Prediction of Activity Spectra for Substances) prediction was carried out for only the two best-selected ligands that showed the best result in inhibiting their respective receptors, MTB RNA polymerase and InhA protein. PASS prediction was conducted by using the PASS-Way2Drug server (<http://www.pharmaexpert.ru/passonline/>) by using canonical SMILES from PubChem server (<https://pubchem.ncbi.nlm.nih.gov/>) (Filimonov et al., 2014). To carry out PASS prediction, Pa (probability "to be active") was kept greater than 70%, since the Pa > 70% threshold gives highly reliable prediction (Geronikaki et al., 1999). In the PASS prediction study, both the possible biological activities and the possible adverse effects of the selected ligands were predicted. The LD50 and Toxicity class were predicted using ProTox-II server (http://tox.charite.de/protox_II/) (Drwal et al., 2014).

3. Results

3.1. Molecular Docking Study and Ramachandran Plot Analysis

All the selected ligand molecules and the controls were docked successfully with their target receptors, MTB RNA polymerase and MTB InhA protein. The controls, rifampicin and isoniazid generated docking scores of -4.813 Kcal/mol (with MTB RNA polymerase) and -6.018 Kcal/mol (with the InhA protein), respectively. 4-hydroxybenzaldehyde generated docking scores of -6.062

Kcal/mol with RNA polymerase and -7.161 Kcal/mol with InhA protein. Benzoic acid showed docking scores of -5.383 Kcal/mol with RNA polymerase and -7.302 Kcal/mol with InhA protein. Bergapten generated docking scores of -5.290 Kcal/mol, when docked against RNA polymerase and -8.068 Kcal/mol with InhA protein. Psoralen generated docking scores of -5.731 Kcal/mol with RNA polymerase and -7.102 Kcal/mol, when docked against InhA protein. And p-hydroxybenzoic acid generated docking scores of -4.617 Kcal/mol with RNA polymerase and -7.538 Kcal/mol with InhA protein. From the docking study, it is clear that 4-hydroxybenzaldehyde generated the lowest score of -6.062 Kcal/mol with RNA polymerase and bergapten generated the lowest score of -8.068 Kcal/mol with InhA protein.

On the other hand, all the ligands and the controls also gave successful results in the MM-GBSA study. In the MM-GBSA study, the ΔG_{Bind} score was determined. Rifampicin and isoniazid generated ΔG_{Bind} scores of -34.317 Kcal/mol and -29.728 Kcal/mol, respectively. 4-hydroxybenzaldehyde generated ΔG_{Bind} scores of -53.070 Kcal/mol with RNA polymerase and -34.240 Kcal/mol with InhA protein. Benzoic acid showed ΔG_{Bind} scores of -40.810 Kcal/mol with RNA polymerase and -40.440 Kcal/mol with InhA protein. Bergapten generated ΔG_{Bind} scores of -42.390 Kcal/mol and -57.590 Kcal/mol with InhA protein. Psoralen generated ΔG_{Bind} scores of -43.150 Kcal/mol with RNA polymerase and -55.330 Kcal/mol with InhA protein. And p-hydroxybenzoic acid generated ΔG_{Bind} scores of -37.53 Kcal/mol with RNA polymerase and -45.740 Kcal/mol with InhA protein. The MM-GBSA study confirmed that 4-hydroxybenzaldehyde also generated the lowest ΔG_{Bind} score of -53.070 Kcal/mol like the docking study with RNA polymerase as well as bergapten generated the lowest ΔG_{Bind} score of -57.590 Kcal/mol with InhA protein.

Bergapten formed the highest number of hydrogen bonds with both RNA polymerase (05) as well as InhA protein (08). Bergapten also interacted with the highest number of amino acids within the binding pocket of RNA polymerase. It interacted with 05 amino acids: Arg 421, Val 422, Leu 1089, Ile 1253 and Gly 1069, when docked against MTB RNA polymerase. On the other hand, it also interacted with 07 amino acids within the bonding pocket of InhA protein: Lys 165, Gly 96, Ile 194, Gly 192, Ala 191, Ile 21 and Met 147. 4-hydroxybenzaldehyde also interacted with 07 amino acids when docked against InhA protein: Met 147, Lys 165, Ile 194, Ile 21, Pro 193, Gly 192 and Ala 191. The docking scores, glide energy and glide ligand efficiency of the controls are listed in **Table 02**. The docking scores, glide energies, glide ligand efficiency scores, ΔG_{Bind} scores, number of hydrogen bonds, interacting amino acids as well as different types of bonds and their distances are listed in **Table 03**. **Figure 03**, **Figure 04** and **Figure 05** illustrate the 2D and 3D representations of the best interaction between the ligands and receptors as well as the various amino acids that take part in the interaction.

Table 02. Results of molecular docking between the controls and their receptors.

Name of the control	Name of the receptors	Docking score/ binding energy (Kcal/mol)	Glide energy (Kcal/mol)	Glide ligand efficiency (Kcal/mol)	MM-GBSA (ΔG_{Bind} Score Kcal/mol)
Rifampicin (PubChem CID: 135398735) (Control-1)	MTB RNA Polymerase (PDB ID: 6M7J)	-4.813	-25.247	-0.503	-34.317
Isoniazid (PubChem CID: 3767) (Control-2)	InhA protein (2NSD)	-6.018	-29.728	-0.602	-25.120

Table 03. Results of molecular docking between ligands and receptors. All the selected ligands were docked successfully against the MTB RNA polymerase and InhA protein.

Name of receptor	Name of ligand	Docking score/ binding energy (Kcal/mol)	Glide energy (Kcal/mol)	Glide ligand efficiency (Kcal/mol)	MM-GBSA (ΔG_{Bind} Score Kcal/mol)	No of hydrogen bonds with amino acids	Interacting amino acids	Bond distance in Å	Types of bonds
MTB RNA Polymerase (PDB ID: 6M7J)	4- hydroxybenz aldehyde (PubChem CID: 126)	-6.062	-21.269	-0.674	-53.070	04	Gln 882	2.56	Conventional
							Lys 1249	4.50	Pi-Alkyl
								3.35	Pi-Cation
							Asp 879	1.65	Conventional
							Trp 1074	4.92	Pi-Pi stacked
3.58	Pi-Pi stacked								

Benzoic acid (PubChem CID: 243)	-5.383	-21.786	-0.598	-40.810	02	Gly 408	2.72	Conventional
						Ala 1224	2.15	Conventional
							4.28	Pi-Alkyl
						Leu 1221	5.28	Pi-Alkyl
						Ile 1253	5.39	Pi-Alkyl
Bergapten (PubChem CID: 2355)	-5.290	-30.331	-0.331	-42.390	05	Arg 421	2.19	Conventional
						Val 422	2.78	Conventional
						Leu 1089	5.02	Pi-Alkyl
							4.93	Pi-Alkyl
						Ile 1253	5.35	Pi-Alkyl
						Gly 1069	2.55	Carbon
Psoralen (PubChem CID: 6199)	-5.731	-26.147	-0.409	-43.150	04	Leu 1089	4.23	Pi-Alkyl
							4.26	Pi-Alkyl
							5.38	Pi-Alkyl
						Cys 1073	5.33	Pi-Alkyl
						Gln 1069	2.66	Carbon
						Lys 420	2.06	Conventional
						Gly 419	2.71	Carbon
							2.84	Conventional
p- hydroxybenz oic acid (PubChem CID: 135)	-4.617	-24.020	-0.462	-37.530	03	Ile 1253	2.14	Conventional
						Leu 1089	2.90	Pi-Sigma
							Lys 420	5.26
						Gly 419	2.47	Pi-Donor
							2.69	Carbon
							2.43	Conventional
4- hydroxybenz	-7.161	-26.863	-0.796	-34.240	04	Lys 165	2.07	Conventional
						Met 147	5.41	Pi-Alkyl

InhA protein (2NSD)	aldehyde (PubChem CID: 126)						Ile 21	5.39	Pi-Alkyl
							Ile 194	2.05	Conventional
							Pro 193	2.86	Carbon
							Gly 192	2.62	Carbon
							Ala 191	5.41	Pi-Alkyl
	Benzoic acid (PubChem CID: 243)	-7.302	-29.106	-0.811	-40.440	03	Ile 21	5.35	Pi-Alkyl
							Ala 191	4.79	Pi-Alkyl
							Pro 193	2.00	Conventional
								2.70	Carbon
	Ile 194	2.18	Conventional						
	Bergapten (PubChem CID: 2355)	-8.068	-35.218	-0.304	-57.590	08	Lys 165	2.14	Conventional
							Gly 96	2.95	Carbon
							Ile 194	3.09	Carbon
								2.81	Carbon
							Gly 192	2.25	Carbon
							Ala 191	2.87	Carbon
								4.40	Pi-Alkyl
							Ile 21	5.08	Pi-Alkyl
							Met 147	5.30	Pi-Alkyl
	5.40	Pi-Alkyl							
Psoralen (PubChem CID: 6199)	-7.102	-32.590	-0.507	-55.330	02	Pro 193	2.88	Carbon	
						Ile 194	1.96	Conventional	
						Ile 21	5.36	Pi-Alkyl	
							5.21	Pi-Alkyl	
						Ala 191	5.17	Pi-Alkyl	
						Met 147	5.22	Pi-Alkyl	
5.25	Pi-Alkyl								
p- hydroxybenz oic acid	-7.538	-32.452	-0.754	-45.740	04	Ile 21	5.39	Pi-Alkyl	
						Ala 191	5.00	Pi-Alkyl	
						Asp 148	1.85	Conventional	

(PubChem CID: 135)						Ile 194	1.79	Conventional
							1.89	Conventional
						Pro 193	2.55	Carbon

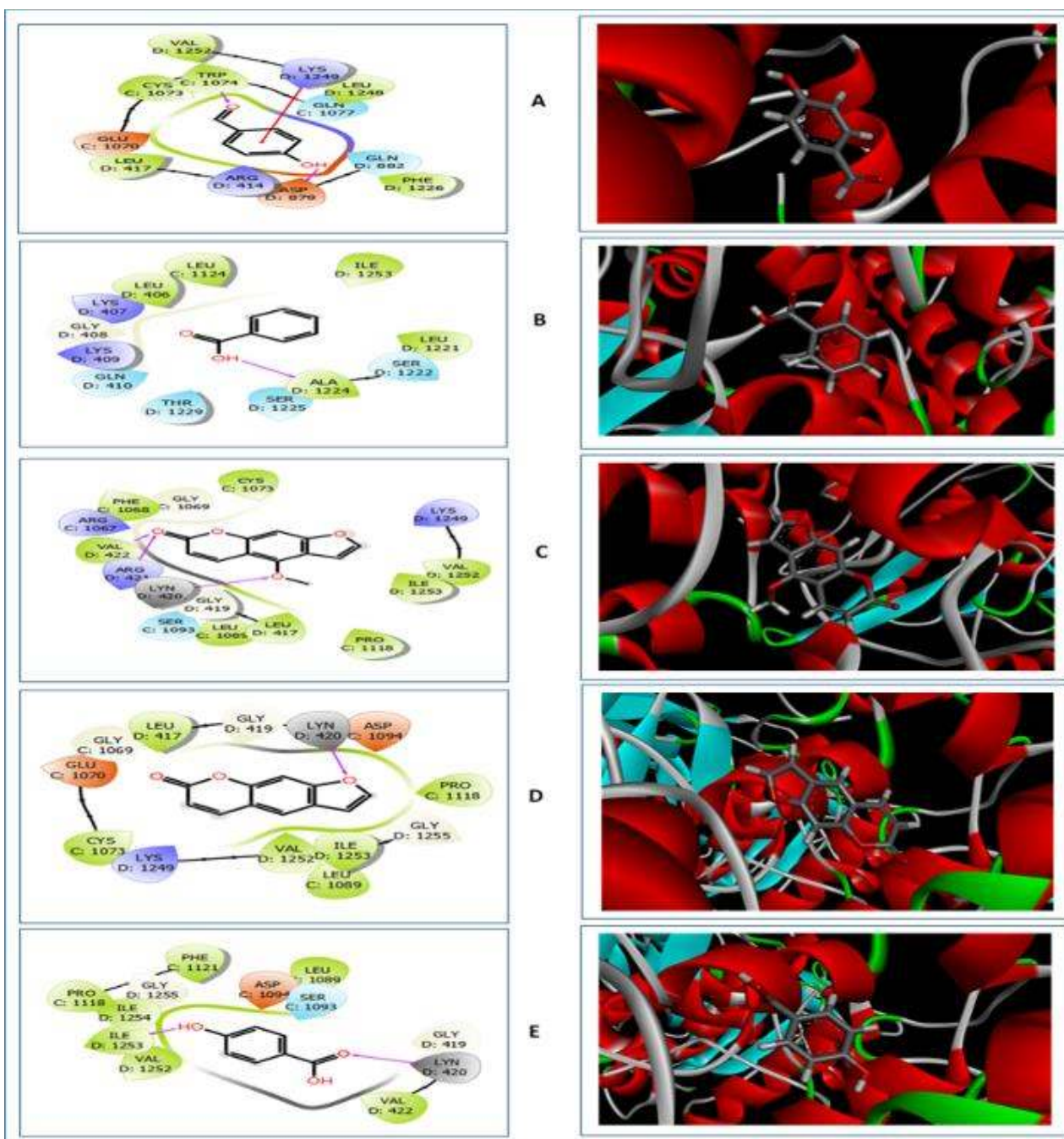


Figure 03. 2D (left) and 3D (right) representations of the best pose interactions between the ligands and the receptor, MTB RNA polymerase. A. interaction between 4-hydroxybenzaldehyde and RNA polymerase, B. interaction between benzoic acid and RNA polymerase, C. interaction between bergapten and RNA polymerase, D. interaction between psoralen and RNA polymerase, E. interaction between p-hydroxybenzoic acid and RNA polymerase. Colored spheres indicates the type of residue in the target: Red-Negatively charged (Asp, Glu), Blue- Polar (Ser, Thr, Gln), Green-Hydrophobic (Ala, Leu, Val, Ile, Trp, Phe, Cys, Pro), Light Purple-Basic (Lys, Arg), Gray-Water molecules, Darker gray-metal atom, Light Yellow- Glycine, Deep Purple- Unspecified molecules and the Grayish circles represent Solvent exposure. Interactions are shown as colored lines- Solid pink lines with arrow- H-bond in target (backbone), Dotted pink lines with arrow- H-bond between receptor and ligand (side-chain), Solid pink lines without arrow- Metal coordination, Green line- Pi-Pi stacking interaction, Green dotted lines- Distances, Partially blue and red colored lines- Salt bridges. Ligands exposed to solvent are represented by the grey sphere. The colored lines show the protein pocket for the ligand according to the nearest atom. Interruptions of the lines indicate the opening of the pocket. In the 3D representations, the proteins are represented in the Solid ribbon model and the ligands are represented in Stick model.

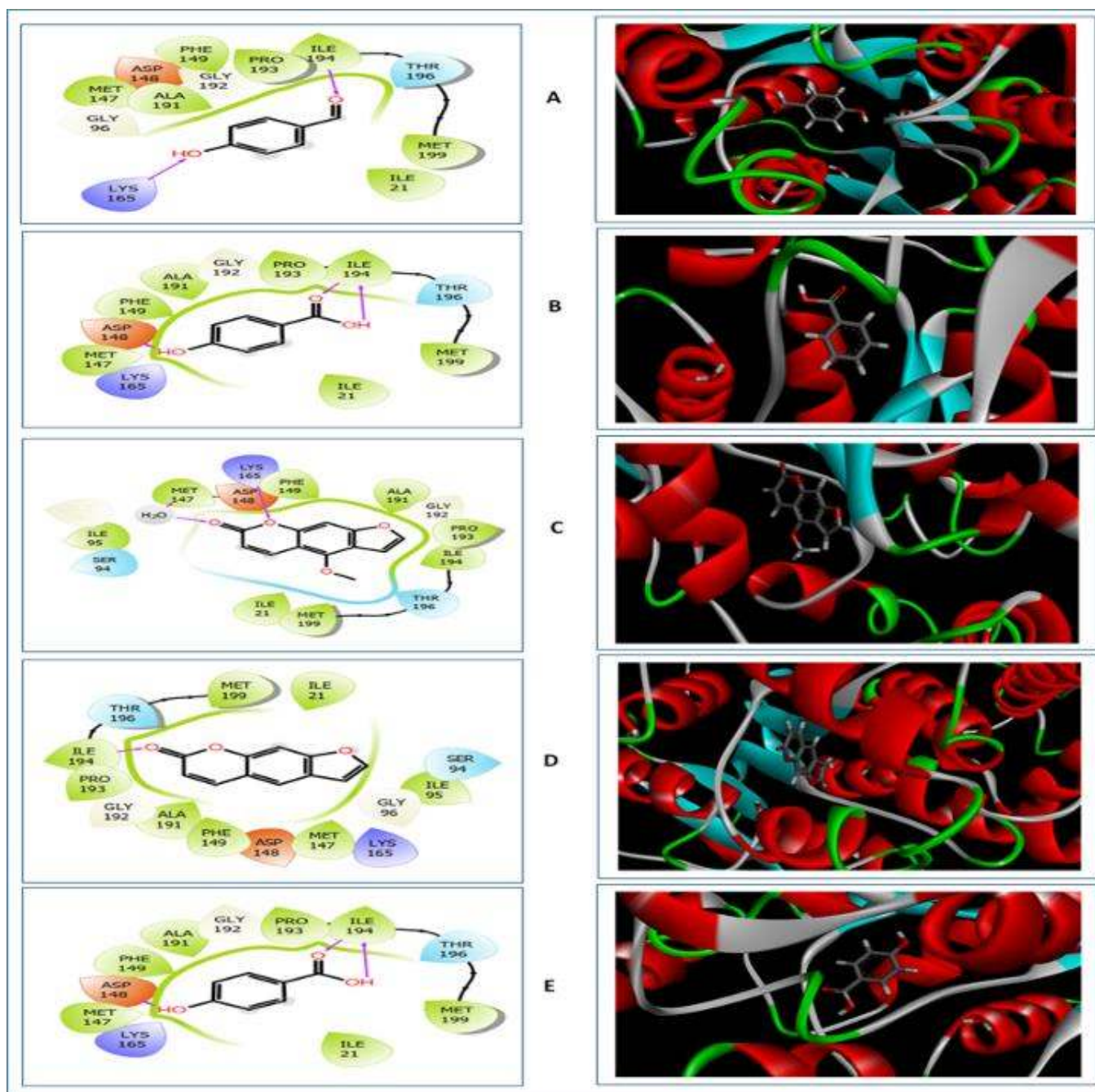


Figure 04. 2D (left) and 3D (right) representations of the best pose interactions between the ligands and the receptor, InhA protein. A. interaction between 4-hydroxybenzaldehyde and InhA protein, B. interaction between benzoic acid and InhA protein, C. interaction between bergapten and InhA protein, D. interaction between psoralen and InhA protein, E. interaction between p-hydroxybenzoic acid and InhA protein. Colored spheres indicate the type of residue in the target: Red-Negatively charged (Asp), Blue- Polar (Ser, Thr), Green-Hydrophobic (Ala, Ile, Phe, Met, Pro), Light Purple-Basic (Lys), Gray- Water molecules, Darker gray-metal atom, Light Yellow-Glycine, Deep Purple- Unspecified molecules and the Grayish circles represent Solvent exposure. Interactions are shown as colored lines- Solid pink lines with arrow- H-bond in the target (backbone), Dotted pink lines with arrow- H-bond between receptor and ligand (side-chain), Solid pink lines without arrow- Metal co-ordination, Green line- Pi-Pi stacking interaction, Green dotted lines- Distances, Partially blue and red colored lines- Salt bridges. Ligands exposed to solvent are represented by grey sphere. The colored lines show the protein pocket for the ligand according to nearest atom. Interruptions of the lines indicate the opening of the pocket. In the 3D representations, the proteins are represented in Solid ribbon model and the ligands are represented in Stick model.

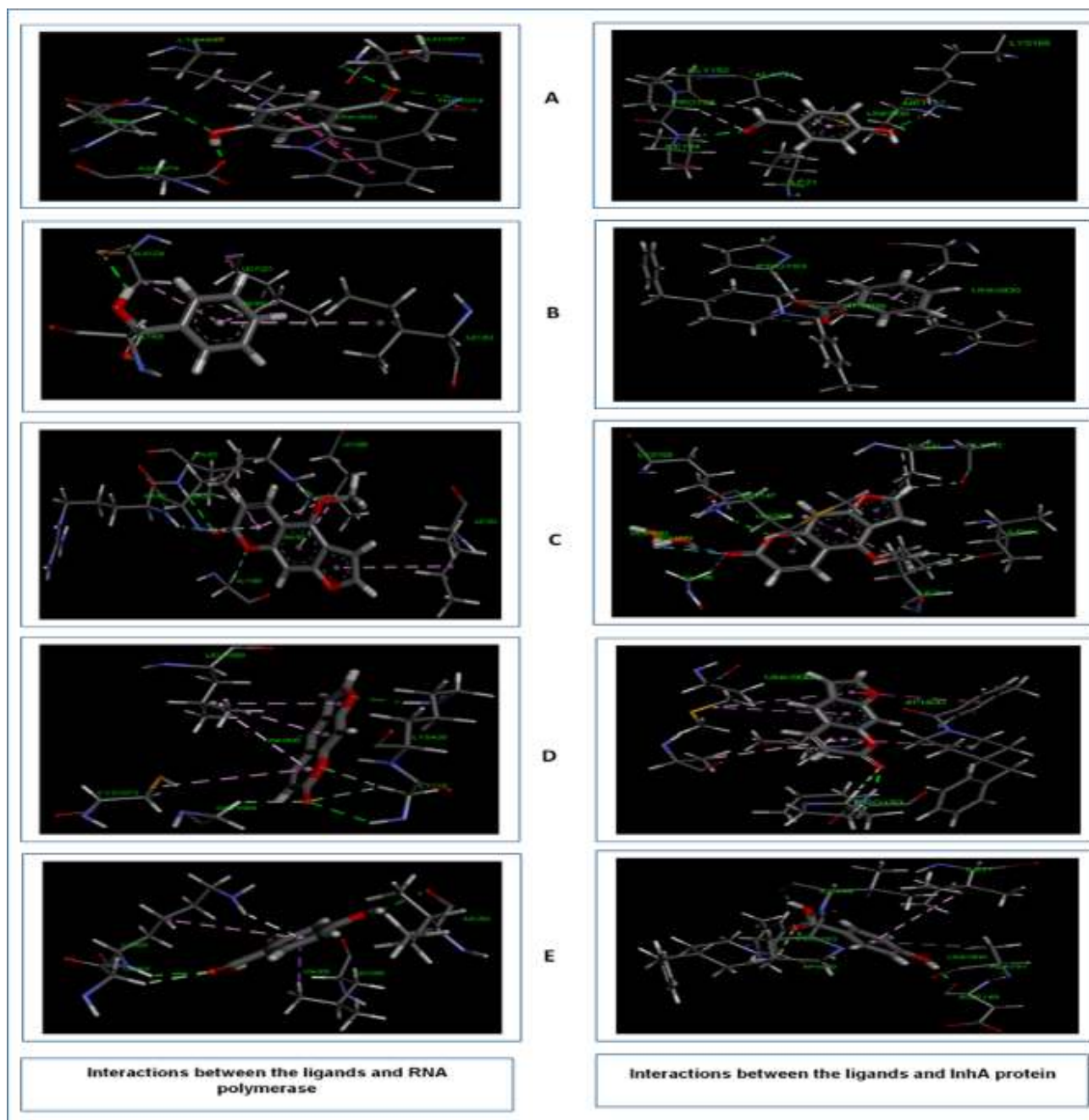


Figure 05. Figure showing the various types of bonds and amino acids that take part in the interaction between the selected ligands and MTB RNA polymerase (left) and InhA protein (right). Interacting amino acid residues of target molecules are labeled in the diagram and dotted lines depict interaction between ligand and receptor. Green dotted lines- Conventional bond, Light pink- Alkyl/Pi-Alkyl interactions, Yellow- Pi-Sulfur/Sulphur-X interaction, Deep pink- Pi-Pi stacked bond, Orange- Charge-Charge interaction, Purple- Pi-Sigma interaction, Red- Donor-Donor interaction. Here, A. 4-hydroxybenzaldehyde, B. benzoic acid, C. bergapten, D. psoralen, E. p-hydroxybenzoic acid.

3.2. Druglikeness Properties

All the ligands obeyed the Lipinski's rule of five: molecular weight (acceptable range: ≤ 500), total number of hydrogen bond donors (acceptable range: ≤ 5), total number of hydrogen bond acceptors (acceptable range: ≤ 10), lipophilicity (LogP, acceptable range: ≤ 5) and molar refractivity (40-130) (Lipinski, 2004). Bergapten had the highest molecular weight of 216.19 g/mol. 4-hydroxybenzaldehyde and benzoic acid showed similar molecular weight of 122.12 g/mol, which was the lowest among all the ligands. The highest consensus Log *Po/w* value was shown by bergapten (2.16) and the lowest value was generated by p-hydroxybenzoic acid of 1.05. However, bergapten showed the lowest LogS value of -2.93 and 4-hydroxybenzaldehyde showed the LogS value of -1.87. Both 4-hydroxybenzaldehyde and benzoic acid had 2 hydrogen bond acceptors each and 1 hydrogen bond donors each. Bergapten had 4 hydrogen bond acceptors and psoralen had 3 hydrogen bond acceptors, however, both of them didn't have any hydrogen bond donors. P-hydroxybenzoic acid had 3 hydrogen bond acceptors and 2 hydrogen bond donors. P-hydroxybenzoic acid possessed the largest topological polar surface area (TPSA) of 57.53 Å².

However, both 4-hydroxybenzaldehyde and benzoic acid showed similar TPSA value of 37.30 Å², which was the lowest TPSA value. Benzoic acid had the highest drug-likeness score of -1.4 and 4-hydroxybenzaldehyde had the lowest score of -6.31. P-hydroxybenzoic acid generated the highest drug score of 0.35 and bergapten generated lowest drug score of 0.10. However, only bergapten was found to be reproductive effective and tumorigenic. And only 4-hydroxybenzaldehyde and benzoic acid were irritant and all the ligands were found to be mutagenic. The values of the drug-likeness properties are listed in **Table 04**.

Druglikeness properties	4-hydroxybenzaldehyde	Benzoic acid	Bergapten	Psoralen	p-hydroxybenzoic acid
Lipinski's rule of five	Yes	Yes	Yes	Yes	Yes
Molecular weight (g/mol)	122.12	122.12	216.19	186.16	138.12
Concensus Log $P_{o/w}$	1.17	1.44	2.16	2.12	1.05
Log S	-1.87	-2.20	-2.93	-2.73	-2.07
Num. H-bond acceptors	2	2	4	3	3
Num. H-bond donors	1	1	0	0	2
Molar Refractivity	33.85	33.40	58.75	52.26	35.42
Ghose	No (3 violations)	No (3 violations)	Yes	Yes	No (3 violations)
Veber	Yes	Yes	Yes	Yes	Yes
Egan	Yes	Yes	Yes	Yes	Yes
Muegge	No (1 violation)	No (1 violation)	Yes	No (1 violation)	No (1 violation)
TPSA (\AA^2)	37.30	37.30	52.58	43.35	57.53
Druglikeness score	-6.3	-1.4	-3.3	-3.2	-1.5
Drug score	0.17	0.21	0.10	0.27	0.35

Reproductive effective	No	No	Yes (High risk)	No	No
Irritant	Yes (High risk)	Yes (High risk)	No	No	No
Tumorigenic	No	No	Yes (High risk)	No	No
Mutagenic	Yes (High risk)	Yes (High risk)	Yes (High risk)	Yes (High risk)	Yes (High risk)

Table 04. Results of the druglikeness property studies of the selected ligand molecules.

3.3. ADME/T Test

The results of the ADME/T test are listed in **Table 05**. In the absorption section, all the selected ligands showed Caco-2 permeability and human intestinal absorption capability. However, all of them were not p-gp inhibitor as well as p-gp substrate. In the distribution section, all of the ligands showed blood-brain barrier permeability. However, p-hydroxybenzoic acid and 4-hydroxybenzaldehyde showed relatively low plasma protein binding capability than the other three ligands. In the metabolism section, 4-hydroxybenzaldehyde, benzoic acid and p-hydroxybenzoic acid were non-inhibitors as well as non-substrate for all the CYP450 isoenzymes. However, due to the unavailability of data in the server, the CYP450 1A2 and CYP450 2C19 substrates were not determined. However, bergapten and psoralen showed quite similar results in the metabolism section with inhibitory effects on the CYP450 1A2, 3A4, 2C9, 2D6 and 2C19. In the excretion section, 4-hydroxybenzaldehyde had the highest half-life of 1.7 h. In the toxicity section, none of

the molecules was hERG blocker and only bergapten was found to be human hepatotoxic as well as Ames positive. However, bergapten and psoralen showed drug-induced liver injury capability.

Table 05. Results of the ADME/T studies of the selected ligand molecules. The ADME/T tests were carried out by online servers, admetSAR (<http://lmmd.ecust.edu.cn/admetSar2>) as well as the ADMETlab (<http://admet.scbdd.com/>).

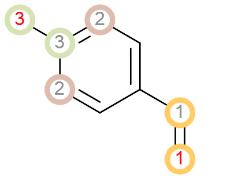
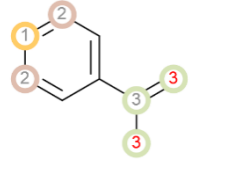
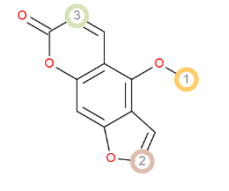
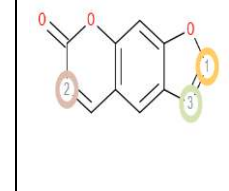
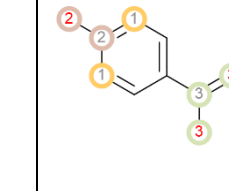
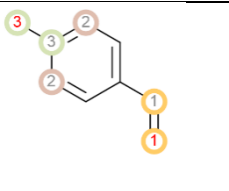
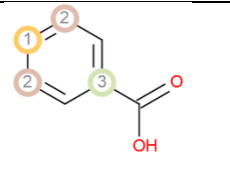
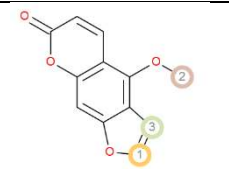
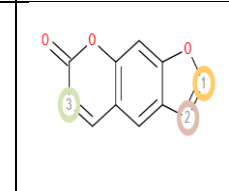
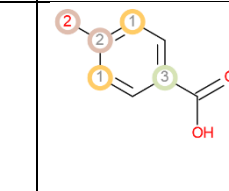
Class	Properties	4-hydroxybenzaldehyde (with probability)	Benzoic acid (with probability)	Bergapten (with probability)	Psoralen (with probability)	P-hydroxybenzoic acid
Absorption	Caco-2 permeability	Positive (0.965)	Positive (0.953)	Positive (0.819)	Positive (0.863)	Positive (0.923)
	Pgp-inhibitor	Negative (0.987)	Negative (0.989)	Negative (0.878)	Negative (0.934)	Negative (0.986)
	Pgp-substrate	Negative (0.989)	Negative (0.997)	Negative (0.924)	Negative (0.951)	Negative (0.990)
	HIA (Human Intestinal Absorption)	Positive (0.990)	Positive (0.981)	Positive (0.991)	Positive (0.988)	Positive (0.983)
Distribution	PPB (Plasma Protein Binding)	Good, 48.4%	High, 77.7%	High, 79.5%	High, 85.3%	Good, 55.6%
	BBB (Blood-Brain Barrier)	Positive (0.848)	Positive (0.781)	Positive (0.883)	Positive (0.852)	Negative (0.7620)
Metabolism	CYP450 1A2 inhibition	Negative (0.752)	Negative (0.853)	Positive (0.974)	Positive (0.910)	Negative (0.975)
	CYP450 1A2 substrate	-	-	-	-	-
	CYP450 3A4 inhibition	Negative (0.915)	Negative (0.982)	Positive (0.795)	Positive (0.767)	Negative (0.949)
	CYP450 3A4 substrate	Negative (0.795)	Negative (0.879)	Negative (0.607)	Negative (0.753)	Negative (0.826)
	CYP450 2C9 inhibition	Negative (0.985)	Negative (0.986)	Positive (0.825)	Positive (0.534)	Negative (0.969)
	CYP450 2C9 substrate	Negative (0.619)	Negative (0.806)	Negative (1.000)	Negative (1.000)	Negative (0.815)
	CYP450 2C19 inhibition	Negative (0.905)	Negative (0.987)	Positive (0.929)	Positive (0.795)	Negative (0.965)

	CYP450 2C19 substrate	-	-	-	-	-
	CYP450 2D6 inhibition	Negative (0.970)	Negative (0.957)	Positive (0.893)	Positive (0.676)	Negative (0.982)
	CYP450 2D6 substrate	Negative (0.729)	Negative (0.885)	Negative (0.815)	Negative (0.844)	Negative (0.873)
	Subcellular localization	Mitochondria	Mitochondria	Mitochondria	Mitochondria	Mitochondria
Excretion	T _{1/2} (h)	1.7	1.5	0.2	1.423	0.773
Toxicity	hERG (hERG Blockers)	Non-blocker (0.198)	Non-blocker (0.169)	Non-blocker (0.344)	Non-blocker (0.298)	Non-blocker (0.238)
	H-HT (Human Hepatotoxicity)	Negative (0.132)	Negative (0.102)	Positive (0.826)	Negative (0.082)	Negative (0.064)
	Ames (Ames Mutagenicity)	Negative (0.006)	Negative (0.078)	Positive (0.882)	Negative (0.072)	Negative (0.068)
	DILI (Drug Induced Liver Injury)	Negative (0.848)	Negative (0.402)	Positive (0.952)	Positive (0.924)	Negative (0.206)

3.4. P450 Site of Metabolism (SOM) Prediction

The P450 SOM prediction was carried out for the five selected ligand molecules and the SOM prediction was performed for CYPs 1A2, 2A6, 2B6, 2C19, 2C8, 2C9, 2D6, 2E1 and 3A4. 4-hydroxybenzoic acid showed 6 SOMs for all the CYP450 isoenzymes, and both bergapten and psoralen showed 3 SOMs each, for all the CYP450 isoenzymes. However, benzoic acid showed 6 SOMs for CYP450 1A2 and CYP450 2C8, 4 SOMs for CYP450 2A6 and 5 SOMs for rest of the CYP450 isoenzymes. P-hydroxybenzoic acid showed 5 SOMs for CYP450 2A6, 6 SOMs for CYP450 2E1 and CYP450 3A4 and 7 SOMs for the rest of the CYP450 isoenzymes. The results of P450 SOM are listed in **Table 06**.

Table 06. The result of P450 site of metabolism prediction of the selected ligand molecules.

Names of P450 isoenzymes	4-hydroxybenzaldehyde	Benzoic acid	Bergapten	Psoralen	P-hydroxybenzoic acid
1A2					
2A6					

2B6					
2C8					
2C9					
2C19					
2D6					
2E1					
3A4					

3.5. Pharmacophore Modelling

In the pharmacophore modelling experiment, all the ligands generated pharmacophore hypotheses while inhibiting both MTB RNA polymerase and InhA protein. 4-hydroxybenzaldehyde generated 4 point hypothesis (features: A1, A2, D3, R4) with MTB RNA polymerase and formed 1 hydrogen bond, 1 pi-cation bond, 3 bad bonds and 1 ugly bond with the binding pocket of the protein. It generated 1 point hypothesis with the InhA protein (feature: A1) and formed 1 pi-pi interaction. Benzoic acid formed 4 point hypothesis (features: A1, A2, D3, R4) while inhibiting the MTB RNA polymerase and formed 1 hydrogen bond and 1 pi-pi interaction within the binding pocket of the receptor. Benzoic acid formed 2 point hypothesis (features: A2, D3) and formed 5 hydrogen bonds and 1 pi-pi interaction within the binding pocket of the receptor protein, InhA protein. Bergapten generated 6 point hypothesis (features: A1, A2, A4, H5, R7, R8) with MTB RNA polymerase and formed 2 bad bonds. However, it generated 3 point hypothesis (features: A2, H5, R7) with the InhA protein and formed 7 hydrogen bonds, 1 pi-pi interaction and 3 bad bonds within the binding pocket of the receptor. Psoralen generated 4 point hypothesis (A1, A2, R4, R6) with MTB RNA polymerase, however, it didn't form any bond with the protein. On the other hand, it generated 3 point hypothesis (features: A1, R4, R6) with InhA protein and formed 1 pi-pi interaction, 1 ugly bond and 3 bad bonds. P-hydroxybenzoic acid generated 4 point hypothesis (A1, A2, D4, R6) with MTB RNA polymerase and formed 2 hydrogen bonds and 3 bad bonds. Moreover, it generated 3 point hypothesis (features: A2, D4, D5) with the InhA protein and formed 1 pi-pi interaction and 3 bad bonds within the binding pocket of the receptor. However, all the ligands also showed a significant number of good bonds with their receptor proteins (**Figure 06** and **Figure 07**).

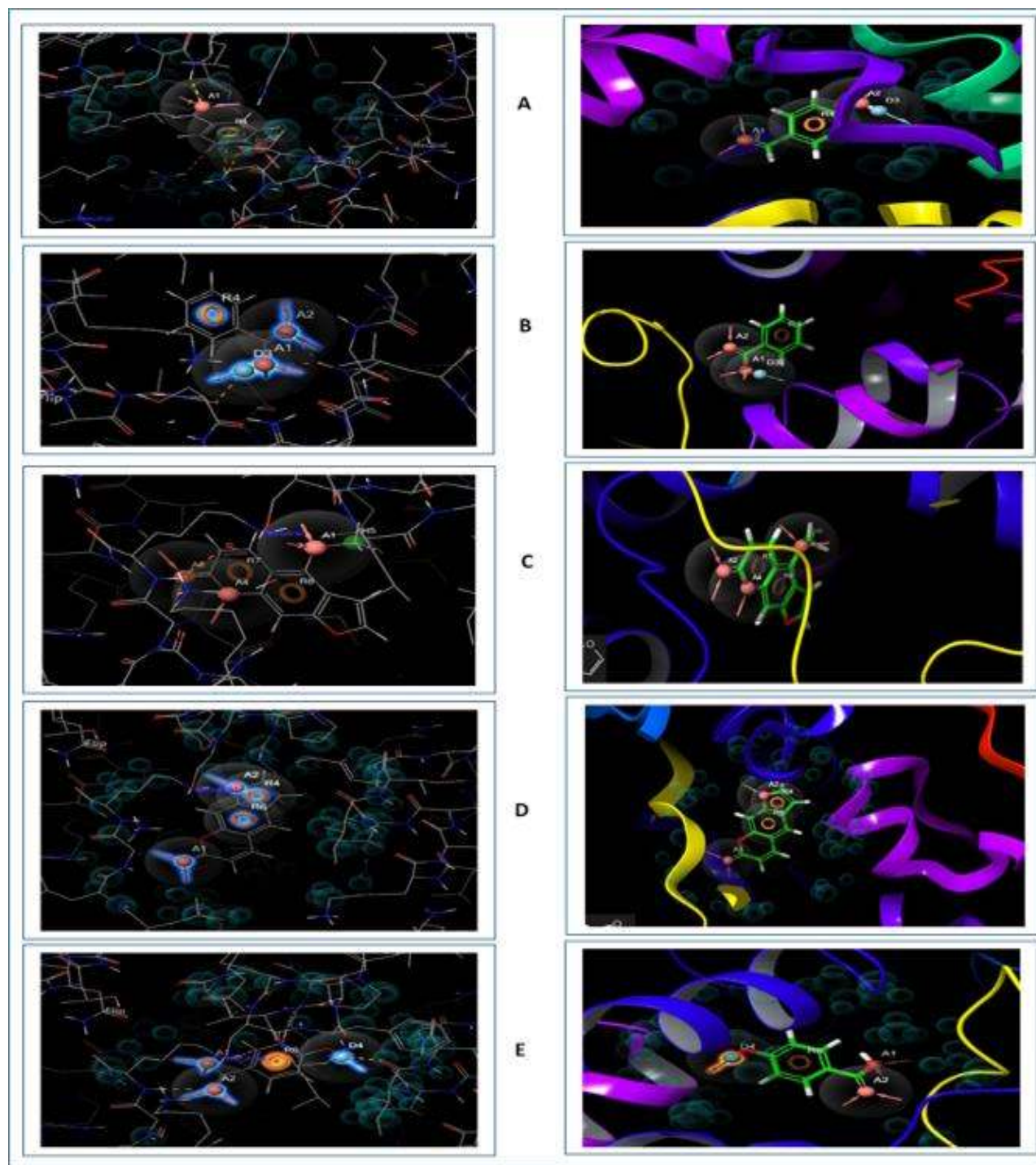


Figure 06. Figure showing the 2D (left) and 3D (right) representations of the pharmacophore hypotheses generated by the ligands while inhibiting the MTB RNA polymerase. Here, A. 4-hydroxybenzaldehyde, B. benzoic acid, C. bergapten, D. psoralen, E. p-hydroxybenzoic acid. The interactions between the ligand and the receptor in the hypothesis were presented by dotted dashed lines, yellow colour- hydrogen bonds and green colour- pi-cation interaction. The bad contacts between the ligands and the pharmacophore are represented. The pharmacophore modelling was carried out by Maestro-Schrödinger Suite 2018-4.

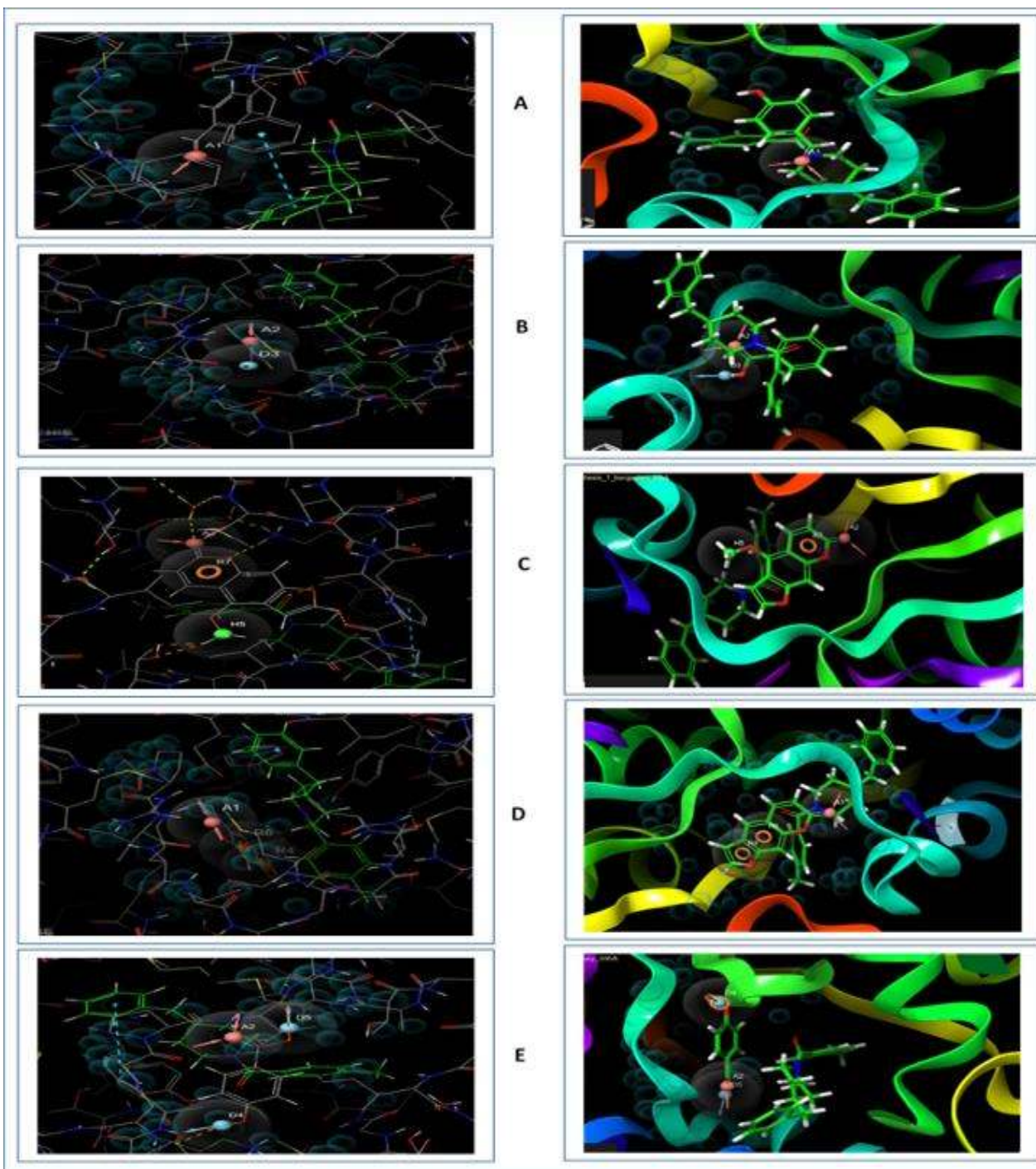


Figure 07. Figure showing the 2D (left) and 3D (right) representations of the pharmacophore hypotheses generated by the ligands while inhibiting the InhA protein. Here, A. 4-hydroxybenzaldehyde, B. benzoic acid, C. bergapten, D. psoralen, E. p-hydroxybenzoic acid. The interactions between the ligand and the receptor in the hypothesis were presented by dotted dashed lines, yellow colour- hydrogen bonds and green colour- pi-cation interaction. The bad contacts between the ligands and the pharmacophore are respresented. The pharmacophore modelling was carried out by Maestro-Schrödinger Suite 2018-4.

3.6. Solubility Prediction

The results of the solubility test of all the ligands are listed in **Table 08**. Bergapten showed the highest QPlogPC16 score of 4.392 and 4-hydroxybenzaldehyde showed the lowest QPlogPC16 score of 2.298. Bergapten also generated the highest QPlogPoct score of 9.129 and the second highest QPlogPoct score was showed by p-hydroxybenzoic acid. However, both benzoic acid and psoralen showed almost similar QPlogPoct results of 4.474 and 4.881, respectively. Bergapten and p-hydroxybenzoic acid also generated the highest and second-highest QPlogPw scores of 8.804 and 6.296, respectively. However, 4-hydroxybenzaldehyde showed the highest QPlogPo/w value of 0.071 and p-hydroxybenzoic acid generated the highest QPlogS score of 0.948. Benzoic acid showed the highest score of CIQPlogS (-0.284) and bergapten generated the lowest CIQPlogS score of -0.883.

Table 08. List of the solubility tests of the selected ligands. The tests were carried out by QikPrep wizard of Maestro-Schrödinger Suite 2018-4. Here,

aPredicted hexadecane/gas partition coefficient (Acceptable range: 4.0 – 18.0); **b**Predicted octanol/gas partition coefficient (Acceptable range: 8.0 – 35.0); **c**Predicted water/gas partition coefficient (Acceptable range: 4.0 – 45.0); **d**Predicted octanol/water partition coefficient (Acceptable range: -2.0 – 6.5); **e**Predicted aqueous solubility, S in mol dm⁻³ (Acceptable range: -6.5 – 0.5); **f**Conformation-independent predicted aqueous solubility, S in mol dm⁻³(Acceptable range: -6.5 – 0.5).

Compound Name	QPlogPC16 ^a	QPlogPoct ^b	QPlogPw ^c	QPlogPo/w ^d	QPlogS ^e	CIQPlogS ^f
4-hydroxybenzaldehyde	2.298	3.081	2.406	0.071	0.241	-0.401
Benzoic acid	2.536	4.474	4.803	-0.193	0.097	-0.284
Bergapten	4.392	9.129	8.804	-0.291	-0.714	-0.883
Psoralen	2.989	4.881	4.697	-0.358	0.075	-0.631
P-hydroxybenzoic acid	3.580	6.697	6.296	-0.813	0.948	-0.364

3.7. DFT Calculations

Table 09 lists the detailed energy of HOMO, LUMO, Gap, hardness, and softness of the compounds. All the molecules successfully generated the HOMO-LUMO structures. The highest HOMO score or energy was showed by bergapten of -0.112 eV and the lowest was generated by p-hydroxybenzoic acid of -0.198 eV. Psoralen generated quite similar score of p-hydroxybenzoic acid of -0.197 eV. 4-hydroxybenzaldehyde and benzoic acid showed similar scores of -0.174 eV. Psoralen generated the lowest LUMO score of 0.039 eV and p-hydroxybenzoic acid generated the highest LUMO score of 0.100 eV. However, p-hydroxybenzoic acid showed the highest gap score of 0.298 eV and bergapten generated the lowest gap score of 0.164 eV. The molecules showed gap scores of quite similar results. 4-hydroxybenzaldehyde, benzoic acid and psoralen showed quite similar hardness scores of 0.114, 0.115 and 0.118 eV respectively. P-hydroxybenzoic acid gave the highest hardness score of 0.149 eV and bergapten showed the lowest hardness score of 0.082 eV. For this reason, bergapten generated the highest softness score of 12.190 and p-hydroxybenzoic acid generated the lowest softness score of 6.710. Moreover, bergapten generated

the highest dipole moment score of 7.186 debye and benzoic acid generated the lowest dipole moment score of 2.217 debye. The HOMO-LUMO representations of the ligands are shown in **Figure 08**.

Table 09. The results of the DFT calculations of the selected ligands.

Name of the ligands	HOMO (in eV)	LUMO (in eV)	Gap (in eV)	Hardness (in eV)	Softness (in eV)	Dipole moment (in Debye)
4-hydroxybenzaldehyde	-0.174	0.053	0.227	0.114	8.770	4.839
Benzoic acid	-0.174	0.055	0.229	0.115	8.690	2.217
Bergapten	-0.112	0.052	0.164	0.082	12.190	7.186
Psoralen	-0.197	0.039	0.236	0.118	8.470	5.272
P-hydroxybenzoic acid	-0.198	0.100	0.298	0.149	6.710	2.524

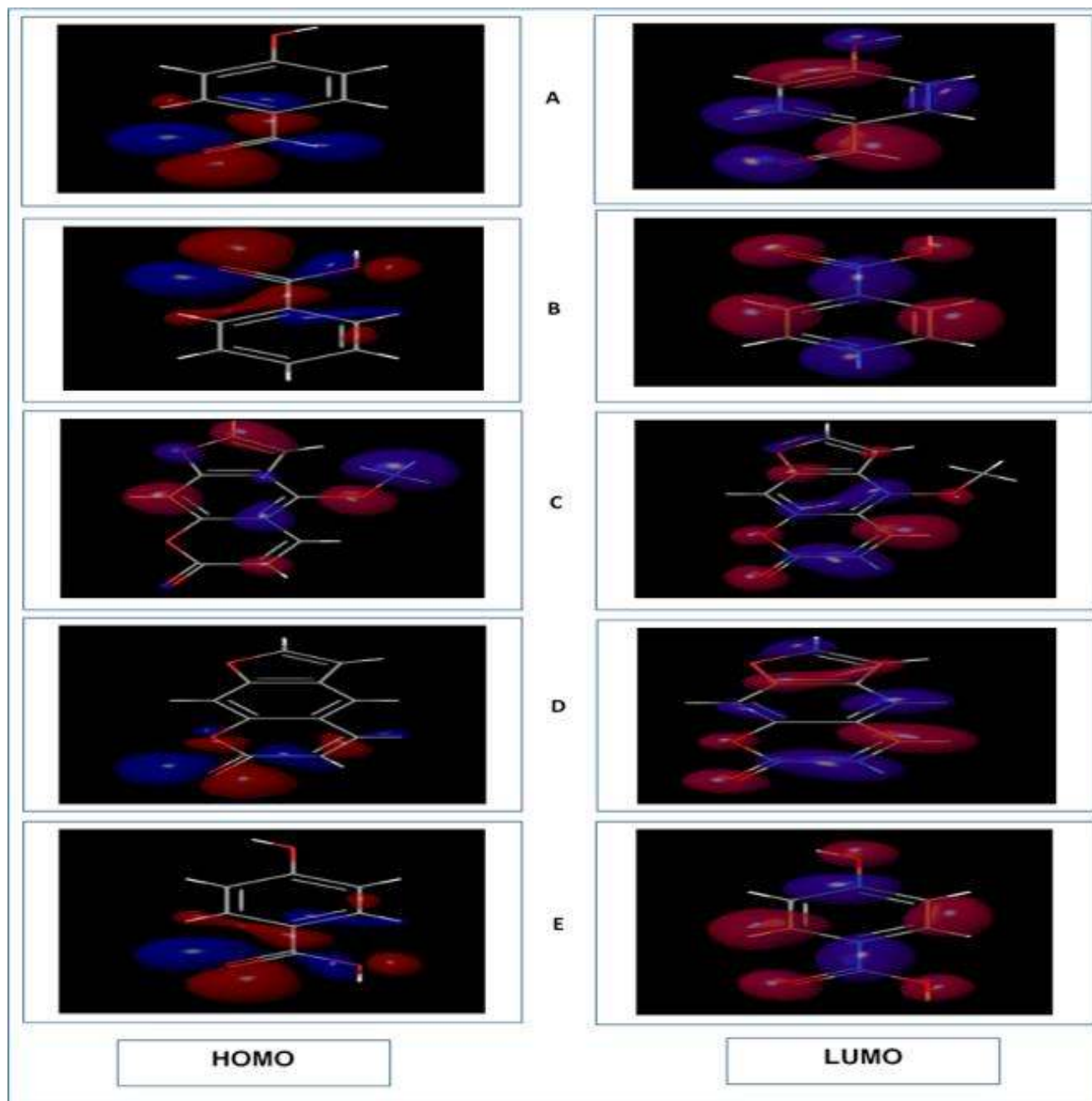


Figure 08. The HOMO (left) and LUMO (right) structures of the selected ligands generated by the Jaguar wizard of Maestro-Schrödinger Suite 2018-4. A. 4-hydroxybenzaldehyde, B. benzoic acid, C. bergapten, D. psoralen, E. p-hydroxybenzoic acid.

3.8. PASS (Prediction of Activity Spectra for Substances) Prediction Study

In the PASS prediction study, the predicted LD50 value and toxicity class of 4-hydroxybenzaldehyde were not determined due to the unavailability of data in the server ProTox II. However, bergapten had the predicted LD50 value of 8100 mg/kg and toxicity class of 6. However, the PASS prediction study was conducted for 10 intended biological activities and 5 toxic effects. To carry out the PASS prediction experiment, $P_a > 0.7$ was kept since this threshold give highly reliable prediction (Geronikaki et al., 1999). Both 4-hydroxybenzaldehyde and bergapten showed activities: aldehyde oxidase inhibitor, CYP2A6 substrate, CYP2A substrate, CYP2E1 substrate and CYP1A2 substrate. However, 4-hydroxybenzaldehyde also showed nitrilase inhibitory activity, thioredoxin inhibitory activity and chymosin activity and bergapten also showed activities: HIF1A expression inhibitor and CYP2A11 substrate. The toxic effects showed by 4-hydroxybenzaldehyde were: weakness, vascular toxicity and fatty liver and bergapten showed the toxic effects: hypothermic and carcinogenic group 3. The results of PASS prediction studies are listed in **Table 10** and **Table 11**.

Table 10. The results of the biological activities PASS prediction study of the selected ligands.

The prediction was conducted by using PASS-Way2Drug server (<http://www.pharmaexpert.ru/passonline/>).

Sl no	Biological activities	4-hydroxybenzaldehyde		Bergapten	
		Predicted LD50: NA		Predicted LD50: 8100 mg/kg	
		Toxicity class: NA		Toxicity class: 6	
		Pa	Pi	Pa	Pi
01	Aldehyde oxidase inhibitor	0.951	0.003	0.747	0.013
02	CYP2A6 substrate	0.854	0.004	0.921	0.003
03	CYP2A substrate	0.854	0.004	0.922	0.004
04	CYP2E1 substrate	0.0843	0.004	0.757	0.004
05	CYP1A2 substrate	0.724	0.008	0.750	0.004
06	Nitrilase inhibitor	0.883	0.002	-	-
07	HIF1A expression inhibitor	-	-	0.732	0.017
08	CYP2A11 substrate	-	-	0.923	0.001
09	Thioredoxin inhibitor	0.757	0.005	-	-
10	Chymosin inhibitor	0.760	0.029	-	-

Table 11. The results of the adverse and toxic effects PASS prediction study of the selected ligands. The prediction was conducted by using PASS-Way2Drug server (<http://www.pharmaexpert.ru/passonline/>).

Predicted adverse and toxic effects	4-hydroxybenzaldehyde		Bergapten	
	Pa	Pi	Pa	Pi
Weakness	0.862	0.011	-	-
Toxic, vascular	0.813	0.015	0.743	0.004
Fatty liver	0.866	0.003	-	-
Hypothermic	-	-	0.730	0.012
Carcinogenic, group 3	0.710	0.021	0.703	0.006

4. Discussions

Molecular docking generates a score based on the binding of ligand and receptor. The higher binding energy represents the lower bonding affinity and vice versa (Sarkar et al., 2019; Sarkar et al., 2020a). Studies have proved that the lowest glide energy corresponds to the best result (Raj and Varadwaj, 2016). The controls, rifampicin and isoniazid successfully docked with their target receptors. The control gave docking scores of -4.813 Kcal/mol and -6.018 Kcal/mol, respectively and glide energies of -25.247 Kcal/mol and -29.728 Kcal/mol, respectively. They generated quite good scores in the docking study.

4-hydroxybenzaldehyde showed the lowest binding energy of -6.062 Kcal/mol when docked against MTB RNA polymerase and bergapten gave the lowest score -8.068 Kcal/mol when docked against InhA protein. However, 4-hydroxybenzaldehyde generated the glide energy of -21.269 Kcal/mol, which was not very good result, since the result was quite high when compared with the other ligands, while docking with MTB RNA polymerase. On the other hand, bergapten, generated

the lowest glide energy of -35.218 Kcal/mol, which is the most acceptable score among the ligands when docked against the InhA protein. For this reason, 4-hydroxybenzaldehyde and bergapten should be the best molecules to inhibit their targets. This is further confirmed by the MM-GBSA study. In the MM-GBSA study, the ΔG_{Bind} score is taken and the lowest (most negative) ΔG_{Bind} Score is always appreciable (Zhang et al., 2017, Ullah et al., 2020a; Sarkar et al., 2020b). 4-hydroxybenzaldehyde generated ΔG_{Bind} Score of -53.070 Kcal/mol, which was the lowest score among all the ligands when docked against MTB RNA polymerase and bergapten generated ΔG_{Bind} score of -57.590 Kcal/mol among the ligands when docked against InhA protein. 4-hydroxybenzaldehyde generated 04 hydrogen bonds when docked against MTB RNA polymerase, which was the second number of most hydrogen bonds (bergapten was the first ligand with 05 hydrogen bonds). On the other hand, bergapten generated the highest number of hydrogen bonds (08) when docked against InhA protein. For this reason, in the molecular docking experiment, 4-hydroxybenzaldehyde and bergapten were the best ligands to inhibit MTB RNA polymerase and InhA protein, respectively (**Table 02** and **Table 03**).

Estimation of druglikeness properties aims to improve the drug discovery and development process. Molecular weight and topological polar surface area (TPSA) affect the permeability of the drug molecule through the biological barrier. Higher molecular weight and TPSA reduce the permeability and vice versa. LogP is expressed in the context of lipophilicity. It is described as the logarithm of partition coefficient of the candidate molecule in organic and aqueous phase. Lipophilicity influences the absorption of the drug molecule inside the body. Higher LogP represents lower absorption and vice versa (Ullah et al., 2019). LogS value influences the solubility of the candidate molecule and the lowest value is always preferred. Moreover, the more the number of hydrogen bonds, the greater the strength of interaction is and vice versa (Lipinski et al., 1997,

Pollastri, 2010; Hubbard and Kamran Haider, 2001). Moreover, according to the Ghose filter, a candidate drug should have logP value between -0.4 and 5.6, molecular weight between 160 and 480, molar refractivity between 40 and 130 and the total number of atoms between 20 and 70, to qualify as a successful drug (Ghose et al., 1999). Veber rule describes that the oral bioavailability of a candidate drug depends on two factors: 10 or fewer numbers of rotatable bonds and the polar surface area which should be equal to or less than 140 \AA^2 (Veber et al., 2002). Furthermore, according to the Egan rule, the absorption of a candidate drug molecule depends on two factors: the polar surface area (PSA) and AlogP98 (the logarithm of partition co-efficient between n-octanol and water) (Egan et al., 2000). And according to the Muegge rule, for a drug like chemical compound to become a successful drug, it has to pass a pharmacophore point filter, which was developed by the scientists (Muegge et al., 2001). According to the druglikeness property experiment, p-hydroxybenzoic acid should be considered as the best molecule since it had quite low molecular weight (138.12 g/mol), the lowest LogP value of 1.05, the highest druglikeness score of -1.5, the highest drug score of 0.35 and no reproductive effectiveness, irritant properties and tumorigenic effects. However, it was found to be a highly mutagenic agent and it had the highest TPSA score of 57.53 \AA^2 . Psoralen also showed good molecular weight of 186.16 g/mol and relatively good LogS value, drug score of 0.27, TPSA score of 43.35 \AA^2 and no reproductive effectiveness, irritant properties and tumorigenic effects were found. However, it didn't perform well like p-hydroxybenzoic acid. Other ligand molecules also performed quite similarly in the druglikeness studies. However, all the ligands obeyed the Lipinski's rule of five. Only bergapten followed the Ghose, Veber, Egan and Muegge rules of druglikeness properties. 4-hydroxybenzaldehyde. Benzoic acid and p-hydroxybenzoic acid violated Ghose and Muegge rules and psoralen violated the Muegge rule.

ADME/T tests evaluate the pharmacological and pharmacodynamic properties of a candidate drug molecule within biological system. Blood brain barrier is very important for those drugs that target primarily the brain cells. Since, the oral delivery system is the most commonly used route of drug administration, therefore, it is expected that the drug is highly absorbed in intestinal tissue. P-glycoprotein protein in the cell membrane facilitates the transport of many drugs. Therefore, its inhibition affects the drug transport. In vitro study of drug permeability test utilizes Caco-2 cell line and its permeability reflects that the drug is easily absorbed in the intestine. Orally absorbed drugs travel through the blood circulation and deposit back to liver. In the liver, they are metabolized by group of enzymes of cytochrome P450 family and excreted as bile or urine. Therefore, inhibition of any of the enzymes of this family might affect biodegradation of the drug molecule (Li, 2001; Guengerich, 1999; Sarkar et al., 2020d). The binding of drugs to the plasma proteins is an important pharmacological parameter which influences the pharmacodynamics of the drugs and their circulation and excretion. A drug's proficiency depends on the degree of its binding with the plasma protein. A drug can diffuse easily through the cell membrane if it binds to the plasma proteins less efficiently and vice versa. Drug half-life defines the time it takes for the concentration or amount of a drug in the body to be reduced by 50%. The greater the half-life of a drug, the longer the drug would stay in the body. For this reason, the half-life determines the doses of drugs (Hossain et al., 2019; Swierczewska et al., 2015; Smalling, 1996; Sarkar et al., 2020c). HERG is a protein in the heart muscle which mediates the rhythm of the heart. HERG can be blocked by many blocking agents. This may lead to the cardiac arrhythmia and sometimes death. Human liver is the primary site of metabolism and it is extremely vulnerable to the harmful effects of various xenobiotic agents. Human hepatotoxicity (H-HT) involves any type of injury to the liver that may lead to organ failure and even death. Ames test is a mutagenicity assay that is

used to detect the mutagenic chemicals. The mutagenic chemicals can cause mutations and also capable of cancer development. Drug induced liver injury (DILI) is the injury to the liver that are caused by administration of drugs. DILI is one of the reasons that may lead to various liver problems (Sanguinetti et al., 1995; Aronov, 2005; Cheng and Dixon, 2003; Mortelmans and Zeiger, 2000; Holt and Ju, 2006).

In the absorption section, all the ligands performed quite similarly, however, based on the probability values, it can be concluded that 4-hydroxybenzaldehyde and benzoic acid are the best performers of the absorption section. In the distribution section, benzoic acid, bergapten and psoralen showed high plasma protein binding capability and all of the ligands were blood brain barrier permeable. Psoralen should be considered as the best performer in the distribution section, based on the probability values. No ligand showed satisfactory results in the metabolism section. However, 4-hydroxybenzaldehyde, benzoic acid and p-hydroxybenzoic acid showed relatively good results since they were not inhibitory to any of the CYP450 isoenzymes. Benzoic acid could be considered as the best ligand in the metabolism section with good probability values. In the excretion section, 4-hydroxybenzaldehyde is the best ligand with the highest half-life of 1.7 hours. In the toxicity section, both 4-hydroxybenzaldehyde, benzoic acid, p-hydroxybenzoic acid showed the best performances since they were not hERG blockers, human hepatotoxic, Ames mutagenic as well as they were also DILI negative. Bergapten was, however, human hepatotoxic, Ames mutagenic and DILI positive and psoralen was only DILI positive.

The Cytochrome P450 (Cyp450) is a family of enzymes and comprises 57 isoforms of P450 enzymes. These enzymes catalyze the phase-I metabolism of almost 90% of the marketed drugs and are heme-containing (Glue and Clement, 1999; Tyzack et al., 2014). The functions of these enzymes are to catalyze the conversion of lipophilic drugs to more polar compounds (Danielson,

2002). Among the 57 isoforms, nine most prevalent isoforms are: CYPs 1A2, 2A6, 2B6, 2C19, 2C8, 2C9, 2D6, 2E1 and 3A4. From the P450 SOM prediction, it can be concluded that all the ligands generated quite sound and similar results.

The Phase pharmacophore perception is a tool of Maestro-Schrödinger Suite 2018-4 that is used in screening of 3D database, pharmacophore modelling and QSAR model development. The engine has 6 types of built-in features and the pharmacophore modelling is mainly carried out based on these 6 types of features: hydrogen bond acceptor (A), hydrogen bond donor (D), negative ionizable (N), positive ionizable (P), hydrophobe (H), and aromatic ring (R). However, the feature number can be increased by customization. The pharmacophore modelling generates a hypothesis which can be used successfully in biological screening for further experiments (Dixon et al., 2006). All the ligand molecules successfully generated the pharmacophore hypotheses. Only psoralen didn't form any bonds with MTB RNA polymerase, however, it generated bonds with the InhA protein. And all other selected ligands formed bonds with both the MTB RNA polymerase and the InhA protein. These hypotheses can be used in various in vitro and in vivo screening of the selected ligand molecules.

All the ligands generated successful solubility results in the solubility test. The acceptable range for QPlogPC16 is 4.0 – 18.0, the acceptable range for QPlogPoct is 8.0 – 35.0, the acceptable range for QPlogPw is 4.0 – 45.0, the acceptable range for QPlogPo/w is -2.0 – 6.5, the acceptable range for QPlogS is -6.5 – 0.5, the acceptable range for CIQPlogS is -6.5 – 0.5 (Hussain and Verma, 2018). Only bergapten gave the QPlogPC16 and QPlogPoct values of 4.392 and 9.129, that are within the acceptable ranges. However, bergapten, benzoic acid, psoralen and p-hydroxybenzoic acid showed QPlogPw values that are within the acceptable range. Moreover, all the ligands showed acceptable values of QPlogPo/w, QPlogS and CIQPlogS. From the solubility test, it can

be concluded that bergapten showed the best results in the solubility test, with its best scores among all the selected ligand molecules (**Table 08**).

Frontier orbitals study is an essential method of understanding the pharmacological properties of various small molecules (Matysiak, 2007). HOMO and LUMO are the globally studied orbitals that help to understand the chemical reactivity and kinetic stability of small molecules. The term 'HOMO' indicates the regions on a small molecule that may donate electrons during a complex formation and the term 'LUMO' indicates the regions on a small molecule that may receive electrons from the electron donating species. The difference between HOMO and LUMO energy is known as gap energy. Gap energy corresponds to the electronic excitation energy. The compound that has the greater orbital gap energy, tends to be energetically unfavourable to undergo a chemical reaction and vice versa (Zhan et al., 2003; Hoque et al., 2015). Moreover, the HOMO-LUMO gap also correlates with the hardness and softness of a molecule (Ayers et al., 2006). From the DFT calculations, it was found that bergapten had the lowest gap energy of 0.164 eV and p-hydroxybenzoic acid had the highest gap energy of 0.298 eV. For this reason, bergapten can be considered as the best ligand molecules since it generated the lowest gap energy and it is very likely to undergo a chemical reaction. Moreover, the lowest gap energy also reflects the lowest hardness score of 0.82 eV and highest softness score of 12.190 eV. Bergapten also had the highest dipole moment of 7.186 debye and p-hydroxybenzoic acid gave the second lowest dipole moment of 2.524 debyes. For this reason, it can be concluded that, bergapten should be the best ligand and p-hydroxybenzoic acid could be the poorest ligand, among the selected ligand molecules.

From the conducted experiments, two ligands, 4-hydroxybenzaldehyde and bergapten were selected as the best ligands to inhibit MTB RNA polymerase (4-hydroxybenzaldehyde) and MTB

InhA protein (bergapten), respectively. 4-hydroxybenzaldehyde showed the best results in the docking experiment while inhibiting MTB RNA polymerase (docking score: -6.062 Kcal/mol and Δ GBind Score: -53.070 Kcal/mol) and bergapten generated the best docking results while inhibiting the MTB InhA protein (docking score: -8.068 Kcal/mol and Δ GBind Score: -57.590 Kcal/mol). In the drug-likeness property experiment, both 4-hydroxybenzaldehyde and bergapten showed fairly good results. In ADME/T test, although, 4-hydroxybenzaldehyde generated one of the best results, however, bergapten showed relatively poor performance in the ADME/T test. In the CYP450 SOM experiment, 4-hydroxybenzaldehyde showed the best results, however, like ADME/T test, bergapten showed poor performance in the CYP450 SOM experiment. On the other hand, in the pharmacophore mapping and modelling, bergapten generated excellent results while inhibiting the InhA protein and 4-hydroxybenzaldehyde also showed quite good result in the pharmacophore modelling experiment while inhibiting MTB RNA polymerase (pharmacophore mapping was not determined). Moreover, in the solubility test and DFT calculation (HOMO-LUMO), bergapten showed the best results, however, 4-hydroxybenzoic acid fairly good performances in these experiments. Both 4-hydroxybenzaldehyde and bergapten generated very good results in some aspects, however, in some other aspects they performed poorly. However, both of their performances in all the experiments were good enough to declare them as the ligands among the selected ligands to inhibit MTB RNA polymerase (4-hydroxybenzaldehyde) and the InhA protein (bergapten). Moreover, the docking study had indicated that, both the two selected best ligands are superior to the controls in terms of the docking score and Δ GBind score of MM-GBSA study. 4-hydroxybenzaldehyde had the docking score of -6.018 Kcal/mol and rifampicin had the docking score of -4.813 Kcal/mol. Moreover, 4-hydroxybenzaldehyde had the Δ GBind score of -53.070 Kcal/mol, whereas, rifampicin had the Δ GBind score of -34.317 Kcal/mol. 4-

hydroxybenzaldehyde had the score that were much lower than the scores of rifampicin. On the other hand, Bergapten was selected as the best ligand to inhibit the InhA protein and it was also far superior than the InhA protein inhibitor or control, isoniazid. Isoniazid had docking score of -6.018 Kca/mol and ΔG_{Bind} score of -25.120 Kcal/mol, whereas, bergapten had much lower scores of -8.068 Kcal/mol and -57.590 Kcal/mol, respectively. For this reason, it can be concluded that, both 4-hydroxybenzaldehyde and bergapten had very performance and good efficiency to inhibit TB, when compared to the widely used drugs that are used to treat TB.

The PASS prediction was study was conducted on only these two best ligands to determine their various biological and toxicological effects. ProTox-II server evaluates the toxicity of a chemical compound and classifies the compound into a toxicity class ranging from 1 to 6. The server classifies the compound according to the Globally Harmonized System of Classification and Labelling of Chemicals (GHS) (36). According to the Globally Harmonized System of Classification and Labelling of Chemicals (GHS), Class 1: fatal if swallowed ($LD_{50} \leq 5$), class 2: fatal if swallowed ($5 < LD_{50} \leq 50$), class 3: toxic if swallowed ($50 < LD_{50} \leq 300$), class 4: harmful if swallowed ($300 < LD_{50} \leq 2000$), class 5: may be harmful if swallowed ($2000 < LD_{50} \leq 5000$) (United Nations. Economic Commission for Europe. Secretariat, 2005). And ProTox-II server adds one more class to the 5 classes, making them 6 classes in total, class VI: non-toxic ($LD_{50} > 5000$) (http://tox.charite.de/prottox_II/index.php?site=home. Accessed on: 09, August, 2019). The predicted LD_{50} value of bergapten was 8100 mg/kg and the toxicity class was 6. For this reason bergapten is non-toxic. The PASS prediction study was carried out for 10 intended biological activities and 5 toxic effects. Both 4-hydroxybenzaldehyde and bergapten showed good biological activities like aldehyde oxidase inhibitor, CYP2A6 substrate, CYP2A substrate, CYP2E1 substrate and CYP1A2 substrate. However, 4-hydroxybenzaldehyde also showed nitrilase inhibitory

activity, thioredoxin inhibitory activity and chymosin activity and bergapten also showed activities: HIF1A expression inhibitor and CYP2A11 substrate. The toxic effects showed by 4-hydroxybenzaldehyde were: weakness, vascular toxicity and fatty liver and bergapten showed the toxic effects: hypothermic and carcinogenic group 3. These toxic effects may interfere with the successful approval and marketing of the drugs. The PASS prediction study had confirmed the superiority of the two best ligands in the toxicity and adverse effects section. For this reason, it can be declared that, both the two selected agents showed satisfactory performances in the tests when compared to the controls.

5. Conclusion

5 agents known to have potential anti-tubercular properties were used to analyse in the experiment. Considering all the parameters, it is clear that, all the plant derived anti-tubercular agents had very good inhibitory activities on the MTB. The various tests of in silico biology, that were used in the experiment, like the molecular docking study, druglikeness property experiment, ADME/T test, pharmacological property analysis, solubility and DFT calculations as well as the PASS prediction study had confirmed that 4-hydroxybenzaldehyde and bergapten were best agents among the selected ligands as well as their superiority over the two commercial, widely used drugs, rifampicin and isoniazid. For this reason, these two agents can be used effectively to fight against tuberculosis. 4-hydroxybenzaldehyde can be acquired from a variety of sources from the nature, like the plant *Cinnamomum kotoense* and bergapten can be acquired from the plant *Fatoua pilosa*. For this reason, these plants can be used effectively to treat tuberculosis. Moreover, in nature, a lot of other

plants can also be found containing these agents. However, more in vivo and in vitro researches should be carried out to finally confirm their activities. Moreover, more researches should be conducted on the other agents to identify their efficacy against TB since they also gave quite good results in the tests carried out in the experiment. Hopefully, this study will help the researchers in identifying the potential anti-tubercular phytochemicals.

Conflict of Interest

Authors state that they have no conflict of interest among themselves.

References

Aronov AM. Predictive in silico modeling for hERG channel blockers. *Drug Discov Today*. 2005;10:149-155.

Ayers PW, Parr RG, Pearson RG. Elucidating the hard/soft acid/base principle: a perspective based on half-reactions. *J Chem Phys*. 2006;124:194107.

Becke AD. Density-functional exchange-energy approximation with correct asymptotic behavior. *Phys Rev A*. 1988;38:3098.

Carel C, Nukdee K, Cantaloube S, Bonne M, Diagne CT, Laval F, Daffe M, Zerbib D. Mycobacterium tuberculosis proteins involved in mycolic acid synthesis and transport localize dynamically to the old growing pole and septum. *PLoS One*. 2014;9:e97148.

Chen FC, Peng CF, Tsai IL, Chen IS. Antitubercular Constituents from the Stem Wood of *Cinnamomum kotoense*. *J Nat Prod*. 2005;68:1318-23.

Chen JJ, Chou TH, Peng CF, Chen IS, Yang SZ. Antitubercular dihydroagarofuranoid sesquiterpenes from the roots of *Microtropis fokiensis*. *J Nat Prod.* 2007;70:202-5.

Cheng A, Dixon SL. In silico models for the prediction of dose-dependent human hepatotoxicity. *J Comput Aid Mol Des.* 2003;17:811-823.

Cheng F, Li W, Zhou Y, Shen J, Wu Z, Liu G, Lee PW, Tang Y. admetSAR: a comprehensive source and free tool for assessment of chemical ADMET properties.

Chiang CC, Cheng MJ, Peng CF, Huang HY, Chen IS. A novel dimeric coumarin analog and antimycobacterial constituents from *Fatoua pilosa*. *Chem Biodivers* 2010;7:1728-36.

Daniel TM. The history of tuberculosis. *Resp Med.* 2006;100:1862-70.

Danielson PB. The cytochrome P450 superfamily: biochemistry, evolution and drug metabolism in humans. *Curr Drug Metab.* 2002;3(6):561-97.

Dixit B. A review on the effects of CMPF binding with Human Serum Albumin. *Bioinformatics Rev.* 2017;3(9):9-18.

Dixon SL, Smodyrev AM, Knoll EH, Rao SN, Shaw DE, Friesner RA. PHASE: a new engine for pharmacophore perception, 3D QSAR model development, and 3D database screening: 1. Methodology and preliminary results. *J Comput Aid Mol Des.* 2006;20:647-71.

Dokorou V, Kovala-Demertzi D, Jasinski JP, Galani A, Demertzis MA. Synthesis, Spectroscopic Studies, and Crystal Structures of Phenylorganotin Derivatives with [Bis (2, 6-dimethylphenyl) amino] benzoic Acid: Novel Antituberculosis Agents. *Helv Chim Akta.* 2004;87:1940-1950.

Dong J, Wang NN, Yao ZJ, Zhang L, Cheng Y, Ouyang D, Lu AP, Cao DS. ADMETlab: a platform for systematic ADMET evaluation based on a comprehensively collected ADMET database. *J Cheminformatics*. 2018;10:29.

Dong Y, Li J, Qiu X, Yan C, Li X. Expression, purification and crystallization of the (3R)-hydroxyacyl-ACP dehydratase HadAB complex from *Mycobacterium tuberculosis*. *Protein Expr Purif*. 2015;114:115-20.

Drwal MN, Banerjee P, Dunkel M, Wettig MR, Preissner R. ProTox: a web server for the in silico prediction of rodent oral toxicity. *Nucleic Acids Res*. 2014;42:W53-8.

Ducasse-Cabanot S, Cohen-Gonsaud M, Marrakchi H, Nguyen M, Zerbib D, Bernadou J, Daffé M, Labesse G, Quémard A. In vitro inhibition of the *Mycobacterium tuberculosis* β -ketoacyl-acyl carrier protein reductase MabA by isoniazid. *Antimicrob Agents Chemother*. 2004;48:242-9.

Egan WJ, Merz KM, Baldwin JJ. Prediction of drug absorption using multivariate statistics. *Journal Med Chem*. 2000;43:3867-77.

Ettehad D, Schaaf HS, Seddon JA, Cooke GS, Ford N. Treatment outcomes for children with multidrug-resistant tuberculosis: a systematic review and meta-analysis. *Lancet Infect Dis*. 2012;12:449-56.

Filimonov DA, Lagunin AA, Glorizova TA, Rudik AV, Druzhilovskii DS, Pogodin PV, Poroikov VV. Prediction of the biological activity spectra of organic compounds using the PASS online web resource. *Chem Heterocycl Com+*. 2014;50:444-57.

Geronikaki A, Poroikov V, Hadjipavlou-Litina D, Filimonov D, Lagunin A, Mgonzo R. Computer aided predicting the biological activity spectra and experimental testing of new thiazole derivatives. *Qsar Comb Sci.* 1999;18:16-25.

Ghose AK, Viswanadhan VN, Wendoloski JJ. A knowledge-based approach in designing combinatorial or medicinal chemistry libraries for drug discovery. 1. A qualitative and quantitative characterization of known drug databases. *J Comb Chem.* 1999;1:55-68.

Glue P, Clement RP. Cytochrome P450 enzymes and drug metabolism—basic concepts and methods of assessment. *Cell Mol Neurobiol.* 1999;19:309-23.

Grange JM, Zumla A. The global emergency of tuberculosis: what is the cause?. *The journal of the Royal Society for the Promotion of Health.* 2002;122:78-81.

Guengerich FP. Cytochrome P-450 3A4: regulation and role in drug metabolism. *Annu Rev Pharmacol.* 1999;39:1-7.

He X, Alian A, de Montellano PR. Inhibition of the Mycobacterium tuberculosis enoyl acyl carrier protein reductase InhA by arylamides. *Bioorgan Med Chem.* 2007;15:6649-58.

Holt MP, Ju C. Mechanisms of drug-induced liver injury. *AAPS J.* 2006;8:E48-54.

Hoque MM, Halim MA, Sarwar MG, Khan MW. Palladium-catalyzed cyclization of 2-alkynyl-N-ethanoyl anilines to indoles: synthesis, structural, spectroscopic, and mechanistic study. *J Phys Org Chem.* 2015;28:732-42.

Hossain S, Sarkar B, Prottoy MN, Araf Y, Taniya MA, Ullah MA. Thrombolytic activity, drug likeness property and ADME/T analysis of isolated phytochemicals from ginger (zingiber

officinale) using in silico approaches. *Modern Research in Inflammation*. 2019 Aug 31;8(3):29-43. DOI: 10.4236/mri.2019.83003

Hubbard RE, Kamran Haider M. Hydrogen bonds in proteins: role and strength. *e LS* 2001.

Hussain A, Verma CK. A Combination of Pharmacophore Modeling, Molecular Docking and Virtual Screening Study Reveals 3, 5, 7-Trihydroxy-2-(3, 4, 5-trihydroxyphenyl)-4H-Chromen-4-One as a Potential Anti-Cancer Agent of COT Kinase. *Indian J Pharm Educ*. 2018;52:699-706.

Lee C, Yang W, Parr RG. Development of the Colle-Salvetti correlation-energy formula into a functional of the electron density. *Phys Rev B*. 1988;37:785.

Li AP. Screening for human ADME/Tox drug properties in drug discovery. *Drug Discov Today*. 2001;6:357-366.

LigPrep, Schrödinger, LLC, New York, NY, 2018-4.

Lim TK. *Hibiscus taiwanensis*. In *Edible Medicinal and Non Medicinal Plants* 2014;381-384.

Lipinski CA, Lombardo F, Dominy BW, Feeney PJ. Experimental and computational approaches to estimate solubility and permeability in drug discovery and development settings. *Adv Drug Deliver Rev*. 1997; 23:3-25.

Lipinski CA. Lead-and drug-like compounds: the rule-of-five revolution. *Drug Discov Today: Technologies*. 2004; 1:337-41.

Matysiak J. Evaluation of electronic, lipophilic and membrane affinity effects on antiproliferative activity of 5-substituted-2-(2, 4-dihydroxyphenyl)-1, 3, 4-thiadiazoles against various human cancer cells. *Eur J Med Chem*. 2007;42:940-7.

McIlleron H, Wash P, Burger A, Norman J, Folb PI, Smith P. Determinants of rifampin, isoniazid, pyrazinamide, and ethambutol pharmacokinetics in a cohort of tuberculosis patients. *Antimicrob Agents Ch.* 2006;50:1170-77.

Moin AT, Sakib MN, Araf Y, Sarkar B, Ullah MA. Combating COVID-19 Pandemic in Bangladesh: A Memorandum from Developing Country. *Preprints.* 2020 May 27. DOI: 10.20944/preprints202005.0435.v1

Molle V, Gulden G, Vilchère C, Veyron-Churlet R, Zanella-Cléon I, Sacchettini JC, Jacobs Jr WR, Kremer L. Phosphorylation of InhA inhibits mycolic acid biosynthesis and growth of *Mycobacterium tuberculosis*. *Mol Microbiol.* 2010;78:1591-605.

Mortelmans K, Zeiger E. The Ames Salmonella/microsome mutagenicity assay. *Mutation research/fundamental and molecular mechanisms of mutagenesis.* 2000;455:29-60.

Muegge I, Heald SL, Brittelli D. Simple selection criteria for drug-like chemical matter. *J Med Chem.* 2001;44:1841-6.

Organic Chemistry Portal. <https://www.organic-chemistry.org/prog/peo>. Accessed on: 10/10/2019.

Parr, R. G., & Yang, W. *Density-Functional Theory of Atoms and Molecules*, vol. 16 of International series of monographs on chemistry. 1989. Oxford University Press. New York.

Pearson RG. Absolute electronegativity and hardness correlated with molecular orbital theory. *PNAS USA.* 1986;83:8440-1.

Pollastri MP. Overview on the Rule of Five. *Curr Protoc Pharmacol.* 2010; 49:9-12.

Raj U, Varadwaj PK. Flavonoids as multi-target inhibitors for proteins associated with Ebola virus: In silico discovery using virtual screening and molecular docking studies. *Interdiscip Sci.* 2016;8:132-41.

Rastogi N, David HL. Mode of action of antituberculous drugs and mechanisms of drug resistance in *Mycobacterium tuberculosis*. *Res Microbiol.* 1993;44:133-43.

Sahin S, Benet LZ. The operational multiple dosing half-life: a key to defining drug accumulation in patients and to designing extended release dosage forms. *Pharm Res.* 2008; 15:2869-77.

Sanguinetti MC, Jiang C, Curran ME, Keating MT. A mechanistic link between an inherited and an acquired cardiac arrhythmia: HERG encodes the IKr potassium channel. *Cell.* 1995;81:299-307.

Sarkar B, Islam SS, Ullah MA, Hossain S, Prottoy MN, Araf Y, Taniya MA. Computational assessment and pharmacological property breakdown of eight patented and candidate drugs against four intended targets in Alzheimer's disease. *Advances in Bioscience and Biotechnology.* 2019 Nov 25;10(11):405. DOI: 10.4236/abb.2019.1011030

Sarkar B, Ullah MA, Araf Y, Das S, Rahman MH, Moin AT. Designing novel epitope-based polyvalent vaccines against herpes simplex virus-1 and 2 exploiting the immunoinformatics approach. *Journal of Biomolecular Structure and Dynamics.* 2020 Aug 6:1-21. DOI: 10.1080/07391102.2020.1803969

Sarkar B, Ullah MA, Araf Y. A systematic and reverse vaccinology approach to design novel subunit vaccines against dengue virus type-1 and human Papillomavirus-16. *Informatics in Medicine Unlocked*. 2020 May 16:100343. DOI: 10.1016/j.imu.2020.100343

Sarkar B, Ullah MA, Islam SS, Rahman MH, Araf Y. Analysis of plant-derived phytochemicals as anti-cancer agents targeting cyclin dependent kinase-2, human topoisomerase IIa and vascular endothelial growth factor receptor-2. *Journal of Receptors and Signal Transduction*. 2020 Aug 12:1-7. DOI: 10.1080/10799893.2020.1805628

Sarkar B, Ullah MA, Prottoy NI. Computational Exploration of Phytochemicals as Potent Inhibitors of Acetylcholinesterase Enzyme in Alzheimer's Disease. *medRxiv*. 2020 Jan 1. DOI: 10.1101/2020.01.04.20016535

Sastry GM, Adzhigirey M, Day T, Annabhimoju R, Sherman W. Protein and ligand preparation: parameters, protocols, and influence on virtual screening enrichments. *J Comput Aid Mol Des*. 2013;27:221-34.

Schneidman-Duhovny D, Nussinov R, Wolfson HJ. Predicting molecular interactions in silico: II. Protein-protein and protein-drug docking. *Curr Med Chem*. 2004;11:91-107.

Schrödinger Release 2015-1: Maestro (2015), Schrödinger, LLC, New York, NY.

Sepkowitz KA. How contagious is tuberculosis?. *Clin Infect Dis*. 1996;23:954-62.

Shah M, Parpio Y, Gul R, Ali A. Educational Needs Of Tuberculosis Patients Based On Their Experiences In Karachi, Pakistan. *i-Manager's Journal on Nursing*. 2015;5:20.

Smalling RW. Molecular biology of plasminogen activators: what are the clinical implications of drug design?. *Am J Cardiol.* 1996;78:2-7.

Sreeramareddy CT, Panduru KV, Verma SC, Joshi HS, Bates MN. Comparison of pulmonary and extrapulmonary tuberculosis in Nepal-a hospital-based retrospective study. *BMC Infect Dis.* 2008;8:8.

Swierczewska M, Lee KC, Lee S. What is the future of PEGylated therapies?. *Expert Opin Emerg Dr.* 2015;20:531-536.

Tyzack JD, Mussa HY, Williamson MJ, Kirchmair J, Glen RC. Cytochrome P450 site of metabolism prediction from 2D topological fingerprints using GPU accelerated probabilistic classifiers. *J Cheminformatics.* 2014;6:29.

Ullah A, Prottoy NI, Araf Y, Hossain S, Sarkar B, Saha A. Molecular Docking and Pharmacological Property Analysis of Phytochemicals from *Clitoria ternatea* as Potent Inhibitors of Cell Cycle Checkpoint Proteins in the Cyclin/CDK Pathway in Cancer Cells. *Computational Molecular Bioscience.* 2019 Sep 6;9(03):81. DOI: 10.4236/cmb.2019.93007

Ullah MA, Johora FT, Sarkar B, Araf Y, Rahman MH. Curcumin analogs as the inhibitors of TLR4 pathway in inflammation and their drug like potentialities: a computer-based study. *Journal of Receptors and Signal Transduction.* 2020 Mar 28;1-5. DOI: 10.1080/10799893.2020.1742741

United Nations. Economic Commission for Europe. Secretariat, 2005. Globally harmonized system of classification and labelling of chemicals (GHS). United Nations Publications.

Veber DF, Johnson SR, Cheng HY, Smith BR, Ward KW, Kopple KD. Molecular properties that influence the oral bioavailability of drug candidates. *J Med Chem.* 2002;45:2615-23.

Visualizer, D.S. (2017) Release 4.1. Accelrys Inc., San Diego, CA.

Yuriev E, Ramsland PA. Latest developments in molecular docking: 2010–2011 in review. *J Mol Recognit.* 2013; 26:215-39.

Zaretski J, Bergeron C, Huang TW, Rydberg P, Swamidass SJ, Breneman CM. RS-WebPredictor: a server for predicting CYP-mediated sites of metabolism on drug-like molecules. *Bioinformatics.* 2012;29:497-8.

Zhan CG, Nichols JA, Dixon DA. Ionization potential, electron affinity, electronegativity, hardness, and electron excitation energy: molecular properties from density functional theory orbital energies. *J Phy Chem A.* 2003;107:4184-95.

Zhang X, Perez-Sanchez, H and C Lightstone F, (2017) A comprehensive docking and MM/GBSA rescoring study of ligand recognition upon binding antithrombin. *Curr Top Med Chem.* 17;1631-39.

Zhang Y, Wade MM, Scorpio A, Zhang H, Sun Z. Mode of action of pyrazinamide: disruption of Mycobacterium tuberculosis membrane transport and energetics by pyrazinoic acid. *J Antimicrob Chemoth.* 2003;52:790-5.

Zoete V, Grosdidier A, Michielin O. Docking, virtual high throughput screening and in silico fragment-based drug design. *J Cell Mol Med.* 2009;13:238-48.